Sediment routing system and sink preservation during the post-orogenic evolution of a retro-foreland basin: The case example of the North Pyrenean (Aquitaine, Bay of Biscay) Basins

Alexandre Ortiz, François Guillocheau, Eric Lasseur, Justine Briais, Cécile Robin, Olivier Serrano, Charlotte Fillon

Journal Pre-proof

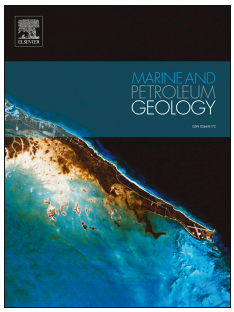

Sediment routing system and sink preservation during the post-orogenic evolution of a retro-foreland basin: The case example of the North Pyrenean (Aquitaine, Bay of Biscay) Basins

Alexandre Ortiz, François Guillocheau, Eric Lasseur, Justine Briais, Cécile Robin, Olivier Serrano, Charlotte Fillon

PII: S0264-8172(19)30521-5

DOI: https://doi.org/10.1016/j.marpetgeo.2019.104085

Reference: JMPG 104085

To appear in: *Marine and Petroleum Geology*

Received Date: 26 July 2019

Revised Date: 7 October 2019

Accepted Date: 9 October 2019

Please cite this article as: Ortiz, A., Guillocheau, Franç., Lasseur, E., Briais, J., Robin, Cé., Serrano, O., Fillon, C., Sediment routing system and sink preservation during the post-orogenic evolution of a retro-foreland basin: The case example of the North Pyrenean (Aquitaine, Bay of Biscay) Basins, *Marine and Petroleum Geology* (2019), doi: https://doi.org/10.1016/j.marpetgeo.2019.104085.

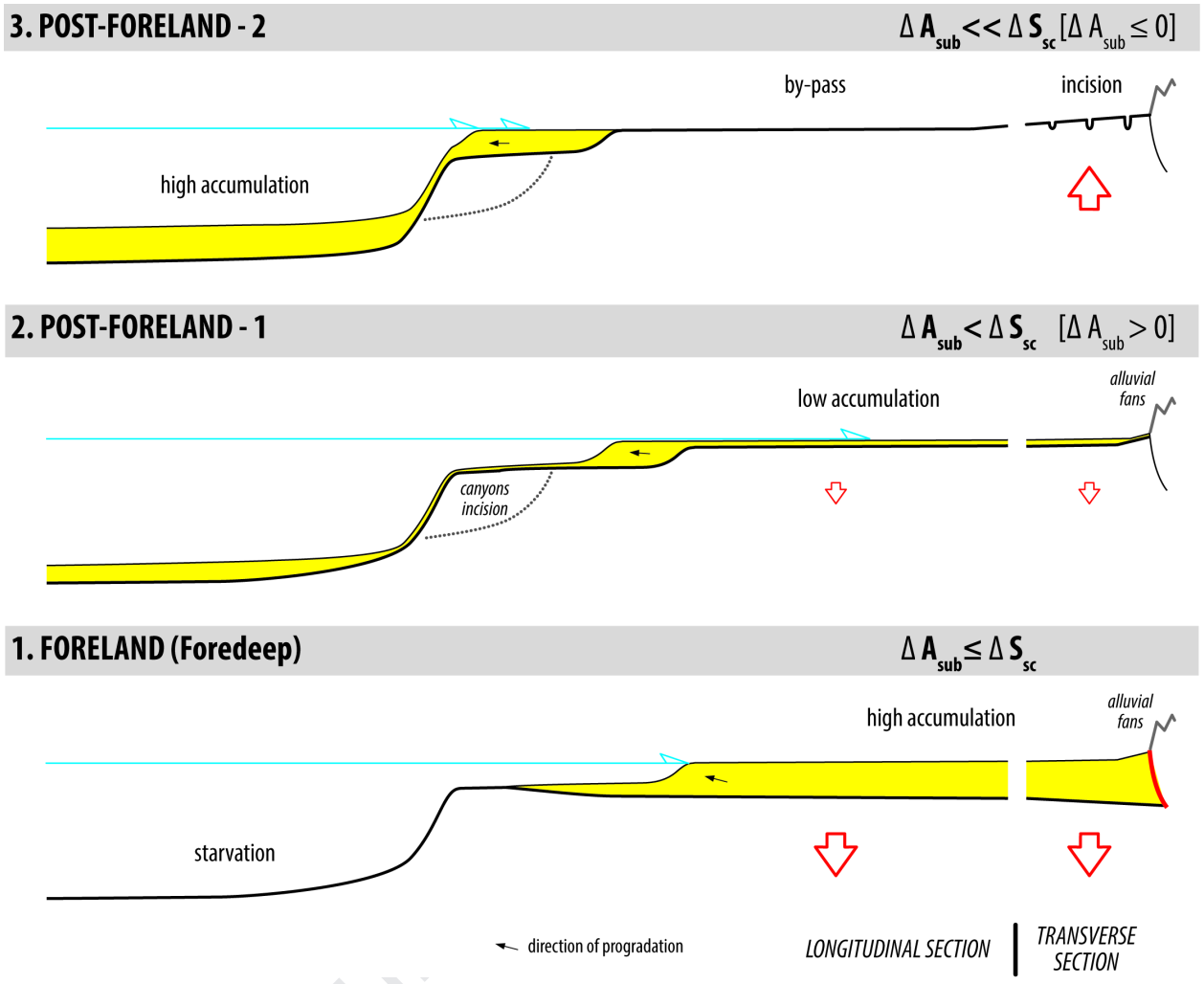
3. POST-FORELAND - 2
$\Delta A_{sub} << \Delta S_{sc}$ [$\Delta A_{sub} \leq 0$]
by-pass
incision
high accumulation
2. POST-FORELAND - 1
$\Delta A_{sub} < \Delta S_{sc}$ [$\Delta A_{sub} > 0$]
low accumulation
alluvial fans
canyons incision
1. FORELAND (Foredeep)
$\Delta A_{sub} \leq \Delta S_{sc}$
high accumulation
alluvial fans
starvation
direction of progradation
LONGITUDINAL SECTION
TRANSVERSE SECTION

Sediment routing system and sink preservation during the post-orogenic evolution of a retro-foreland basin: the case example of the North Pyrenean (Aquitaine, Bay of Biscay) Basins

Alexandre Ortiz[1*], François Guillocheau[1], Eric Lasseur[2], Justine Briais[2], Cécile Robin[1], Olivier Serrano[2], Charlotte Fillon[3]

1 : Univ Rennes, CNRS, Géosciences Rennes - UMR 6118, 35000 Rennes, France

2 : BRGM (French Geological Survey), 45060 Orléans Cedex 2, France

3 : TOTAL, Research and Development, 64018 Pau Cedex, France

*Corresponding author.

Email address : alexandre.ortiz@univ-rennes1.fr

Abstract

We investigated here the evolution of the sediment routing system, i.e. the sediment transport and deposition evolution along successive depositional topographies and environments, and the sink (i.e. deposited sediments) preservation in a foreland basin from the period of mountain belt shortening to its post-orogenic stage. The studied system is the

North Pyrenean retro-foreland basin from 50 Ma to today which is, composed of a subsiding platform (the Aquitaine Basin) fed by the erosion of the Pyrenees passing laterally to a slope and a deep-sea plain (the Bay of Biscay deep basin), the ultimate area of deposition. This study is based on a double seismic stratigraphic and structural analysis of an extensive seismic dataset and on an age model of the sediments combining biostratigraphy, orbitostratigraphy and sequence stratigraphy with a time resolution of 0.1 Ma.

Four major periods of deformation corresponding to a single or a set of stratigraphic sequence boundaries were characterized. The Pyrenean shortening decrease may be recorded by a basin-scale uplift at 49.8 Ma (Late Ypresian). The paroxysm of the piggy-back shortening and related uplift is dated at 35.8 Ma (Priabonian). The end of the Pyrenees shortening (transition to post-orogenic conditions) is well dated between 27.1 and 25.2 Ma (Chattian). A major West European scale deformation of possible mantle origin uplifted the basin from 16.4 to 10.4 Ma (Late Burdigalian to Early Tortonian).

These major periods of deformations controlled the sink preservation at the first order through the ratio between the accommodation space created by subsidence on the Aquitaine platform (A_{sub}) and the siliciclastic sediment supply coming from the erosion of the Pyrenees (S_{sc}). A general model is proposed. At the time of the foreland basin when $\Delta A_{sub} \leq \Delta S_{sc}$, most of the sediments are preserved on the platform as a progradational-aggradational wedge (up to 25.2 Ma here). At the time of the post-foreland evolution when $\Delta A_{sub} < \Delta S_{sc}$,

most of the sediments are transferred to the deep-sea plain with few preservations on the platform and when $\Delta A_{sub} << \Delta S_{sc}$ with $\Delta A_{sub} \leq 0$, all of the sediments are transferred to the deep-sea plain as deep-sea fans and fluvial by-pass or erosion is the dominant process on the platform.

The continental sediment routing system is mainly provided along nearly flat alluvial plains with extensive lakes and/or humid zones, i.e. the local base levels of the alluvial fans. The Aquitaine retro-foreland was never overfilled.

Keywords: Foreland, Post-orogenic, Sediment routing, Sink, Pyrenees, Aquitaine Basin, Bay of Biscay Basin

1. Introduction

Plate flexure that results from tectonic loading by collisional orogens creates accommodation space that is filled by sediments thereby creating foreland basins (Dickinson, 1974; Beaumont, 1981; Allen and Allen, 2013). In doubly-vergent belts, there are two types of foreland according to their position with regards to the orogenic wedge

(Johnson and Beaumont, 1995; Naylor and Sinclair, 2008): (i) pro-foreland on the lower (underthrusted) lithosphere and (ii) retro-foreland on the upper (overriding) lithosphere. The dynamic topography due to mantle flow generated by slab subduction may add an additional component of the subsidence in foreland basins (Mitrovica et al., 1989; Gurnis, 1992; DeCelles and Giles, 1996).

The first-order *stratigraphic architecture* of foreland basins is well understood since the work of Fleming and Jordan (1989). The main parameters controlling the basin infill are : thrust loading, flexural rigidity of the continental lithosphere, erosion rates of the mountain belt, 'depositional styles' (e.g. Sinclair et al., 1991; Sinclair and Allen, 1992). They control whether foreland basins are underfilled, balanced or, overfilled according to the balance with subsidence and sediment flux (Covey, 1988). Some authors replaced foreland infilling in a sequence stratigraphy framework (Posamentier and Allen, 1993). Lastly, some others integrated the effect of both flexural and dynamic topography-induced subsidence (Catuneanu et al., 1997) with the concept of reciprocal stratigraphy.

The *sediment routing* system in foreland basins (Allen, 2017) is highly dependent on the basin physiography. Most forelands are exoreic systems connected to the sea. In that case, the connection of the drainage system to the ocean (e.g. Miall, 1981)may be (1) a lateral

evolution of the foreland basin to a passive margin in a single subsiding domain (e.g. the Western Interior Basin, the foreland basin of the Rocky Mountains passing southward to the passive margin of the Gulf of Mexico) or (2) two disconnected basins, the foreland and passive margin basins, with a non subsiding domain in between (e.g. Amazon foreland and the Fos de Amazonas passive margin in Brazil). During the last stage of the foreland evolution when part of the basin can be transported (piggy-back), the effect of the growing thrusts (lateral and frontal ramps) on the drainage system is well understood in the South Pyrenean foreland (e.g. Vergés and Garcia-Senz, 2001). Recently some studies have focused on the quantification of the sediment routing system and the sediment mass balance ('source-to-sink' approach) in the South Pyrenean foreland basin (Michael et al, 2013, 2014ab; Armitage et al., 2015), examining the role of catchments uplift and/or surface runoff variations, in addition to the effect of relative sea level variations on sediment infilling.

Little attention has been paid to the post-orogenic evolution of the foreland basins. The best documented example is the Alpine 'Molassic' Basin in Switzerland (Schlunnegger and Mosar, 2011; Willett and Schlunnegger, 2010) for which the transition to post-foreland conditions is an overall uplift of the basin at the time of the Jura wedge main activity. These authors emphasized the importance of the boundary conditions in controlling the end of the

foreland subsidence period: the mechanical properties of the lithosphere, the existence of a decollement level and the importance of emerging relief around.

By further investigating how the sink is preserved in the North-Pyrenean foreland basin we propose a model of sediment response to the syn-/post- orogenic transition. The studied system is the retro-foreland of the Pyrenees (Fig. 1), the Aquitaine Basin and its lateral equivalent, the deep Bay of Biscay Basin – the ultimate area of deposition on intermediate to oceanic crust.

Here, we present a seismic stratigraphic analysis of an extensive 2D seismic dataset supplemented by wells (petroleum and water resources). This analysis is based on (1) an age model of the sediments using a new method of dating that combine biostratigraphy (published and new data), orbitostratigraphy and sequences stratigraphy, (2) a geometrical reconstruction of the basin based on seismic stratigraphy and structural analysis (2D sections and isopach maps), (3) a reconstruction of the successive depositional profiles using facies sedimentology and (4) a characterization of the tectonic structures.

2. Geological setting

2.1. Main topographic and structural features (Fig. 1)

115

116 The studied area is subdivided into three main physiographic units. Eastward, the
117 *Aquitaine Basin*, bounded to the south by the Pyrenees and to the north by the French
118 Massif Central (exhumed Variscan basement) extends offshore up to the shelf-break.
119 Westward, the *Bay of Biscay deep basin*, with a mean water depth of 4000 – 4500 m and
120 bounded to the north by the South Armorican Margin and to the south by the Cantabrian
121 (North Iberian) Margin, is located on both an hyperextended continental crust and an
122 oceanic crust. In between, the *Landes Plateau* is a step (more than 100 km wide), that is
123 bounded by quite steep slopes (maximum values: 13-15.5°) eastward and westward, by, the
124 Cap Ferret Canyon northward and the Cap Breton Canyon southward.
125 The continental basement of the Aquitaine Basin is made of late orogenic Variscan
126 structures (Carboniferous-Permian) and little deformed Early Paleozoic rocks (Le Pochat,
127 1984; Paris and Le Pochat, 1994). The key structural feature is the occurrence of a Triassic
128 deposits south of the so-called Celtaquitaine flexure' or hinge line, which is in fact onlap limit
129 of the Late Triassic salt sediments (Bourouilh et al., 1995, Fig. 1).Evaporitic deposits
130 controlled Cretaceous to Cenozoic salt tectonic and diapiric features both in the southern
131 Aquitaine Basin and on the Landes Plateau. The most remarkable ones are the Arzacq,
132 Tartas, Tarbes and Mirande Subbasins bounded by blind thrusts (Audignon and
133 Maubourguet Ridges) or transcurrent zones. The Parentis Subbasin, a rifted basins aborded

in the Early Cretaceous (Mathieu, 1986; Ferrer et al., 2012; Tugend et al., 2015), is located in the middle part of the Aquitaine Basin, mainly offshore. The Bay of Biscay deep basin is characterized by highs (or banks) resulting from the inversion of extensional blocks both to the north (e.g. Gascogne Dome and Trevelyan High - Thinon, 1999; Thinon et al., 2001, 2002) and to the south with the Le Danois Bank, inversion of the Asturian Basin (Cadenas et al., 2017) bounded by the Biscay wedge front (Fernández-Viejo et al., 2012). The North Iberian Biscay wedge front and the North Pyrenean front are connected along a faulted zone, the Santander "soft" transfer zone (Roca et al., 2011) corresponding to the sharp westward limit of the Landes Plateau and controlling the location of the north-south trending Torrelavega and Santander Canyons.

2.2. Evolution of the Pyrenees and its foreland basins

The Pyrenees mountain range and its westward equivalents the Basque-Cantabrian Mountains result from the compression and inversion of the hyperextended Eurasian lithosphere during Albian times since 85 Ma (e.g. Lagabrielle et al., 2010; Masini et al., 2014; Clerc et al., 2016; Saspiturry et al., 2019). Even if the Pyrenean Belt is not cylindrical (Chevrot et al., 2018), its structure can be described as a wedge of Eurasian lithosphere over the Iberian lithosphere plunging to the north (e.g. Roure et al. 1989; Teixell et al., 2018).

153

154 The inversion tectonics started at the time of the Africa-Eurasia convergence with the
155 Iberian microplate at the end of the Santonian (83.6 Ma - e.g. Schettino and Turco, 2011).
156 Plate kinematic constraints (Roest and Srivastava, 1991) impose an end of convergence
157 between Iberia and Eurasia not no later than chron 6c, i.e. around the Oligocene-Miocene
158 boundary (22.6-24.1 Ma, Gradstein et al., 2012). The total amount of shortening varies
159 along-strike: 82 km to the East (Verges et al., 1995) , 142 km to 165 km in the center
160 (Beaumont et al., 2000, Mouthereau et al., 2014) and 114 km to the West (Teixell et al.,
161 2016). The measurements of the shortening rates through time along different segments of
162 the mountain belt (Mouthereau et al., 2014; Teixell et al., 2016 –see synthetic Fig. 12) shows
163 maximum rates from 66 Ma (base Palaeocene) to 48 Ma (base Middle Eocene) (32 km of
164 shortening for Mouthereau et al. vs. 54 km for Teixell et al.) followed by a decrease up to 20
165 – 15 Ma. The collision occurred synchronously along strike. However, the exhumation was
166 delayed toward the west due to the progressive closure of a larger Early Cretaceous domain
167 to the west (Vacherat et al., 2017). Numerical modelling (Curry et al., 2019 - see Fig. 12) of
168 the lithospheric flexure due to loading by the Pyrenees suggests a sharp topographic growth
169 of the Pyrenees during the Priabonian (38-34 Ma – up to 2 to 3 km of maximum elevation)
170 reaching its maximum (3.5 km) around the Oligocene-Miocene boundary (23 Ma). Isotopic
171 studies (Huyghe et al., 2012) suggest an earlier uplift of the eastern mountain belt during

Middle Eocene times.Curry's model (2019) is in agreement with thermochronological data (e.g. Fitzgerlad et al., 1999; Sinclair et al., 2005; Fillon and van der Beek, 2012; Bosch et al., 2016) which showed an acceleration of the exhumation during late Eocene-Oligocene times.

This convergence results in the formation of a major pro-foreland basin to the south, the South Pyrenean Basin and a retro-foreland - to the north, the Aquitaine (Carcassonne) Basin. The South Pyrenean Basin was initiated during the Late Santonian (around 84 Ma – Puigdefabregas and Souquet, 1986) and is transported as a piggy-back basin at the base of the Ypresian (Puigdefabregas and Souquet, 1986; Vergés et al., 2002). This basin opens up toward the Atlantic and became an endoreic system at time of the uplift of the Basque-Cantabrian Mountains, i.e. during the Late Eocene (37 Ma – Gomez et al., 2002).

Along the Bay of Biscay the former Lower Cretaceous extensional blocks of the South Armorican Margin are inverted during early Upper Cretaceous, Palaeocene and Upper Eocene times, this last being the major one with a significant dextral strike-slip component (Thinon, 1999; Thinon et al., 2001, 2002). The southern part, the Asturian Basin (Le Danois Bank), is inverted and thrusted from the Upper Eocene to the Eocene-Oligocene boundary (paroxysm of the deformation - Gallastegui et al., 2002).

Many studies focussing on the Pyrenees mountain belt and surrounding domains (Desegaulx et al., 1991; Angrand et al., 2018; Cochelin et al., 2018; Espurt et al., 2019)

conclude on the importance of structural inheritance of previous deformation events, e.g. the late Variscan (Carbonifereous to Permian) orogeny and Lower Cretaceous extension. The most important event is the Albian lithospheric thinning that controlled the segmentation of the foredeep into numerous subbasins during the Palaeogene (Angrand et al., 2018). The second inheritance effect of the Albian rifting is the occurrence of a rigid block located between the Parentis and Arzacq-Mauleon rifts, the Landes High, which extends from the Landes Plateau to the southwestern part of the Aquitaine Basin (Tugend et al., 2014). For the late Variscan orogenic deformations, although the role of the inherited structure is clearly demonstrated on the 2D sections (Espurt et al., 2019), no clear plan-view data (maps) are available and the meaning of the N20° faults, such as the Pamplona and Toulouse Faults (with possible other ones in between), is still unclear.

2.3. Cenozoic stratigraphy, palaeogeography and deformation of the retroforeland of the Aquitaine Basin

We mainly focused on the Aquitaine Basin in the present study. . Little is known on the stratigraphy of the Bay of Biscay due to (i) the absence of accurately located deep-sea-drillings (e.g. DSDP site 128 leg 12 drilled north of Galicia on the Cantabria Seamount) and by

(ii) the few studies available (e.g. Cremer, 1983) that extrapolate ages of the deep sediments from the shelf wells.

At the first order the Cenozoic infilling of the Aquitaine Basin result from an overall progradation from east (Carcassonne- Corbières area) to west (Atlantic Margin) due to deltas or carbonate platforms prograding wedges with clinoforms that are hundreds of meters tall (Winnock et al., 1973; Dubreuilh et al., 1995). Despite numerous stratigraphic studies (e.g. Cavelier et al., 1997; Sztrákos et al., 1997, 1998, 2010; Sztrákos and Steurbaut, 2017), the lithostratigraphic nomenclature and dating are still quite contradictory. Few 3D reconstructions based on sequence stratigraphic analysis are available (Serrano, 2001; Serrano et al., 2001 for the northern part of the foredeep). Nevertheless, the history of the Cenozoic basin infilling can be summarized in five steps, following a Late Cretaceous (Campanian-Maastrichtian) early phase of flexuration (e.g. Ford et al., 2016).

- From the *Danian* to *Thanetian* (*66-56* Ma), large shallow-water carbonate platforms covered the southern part of the Aquitaine Basin (Sztrákos et al., 1997; Serrano, 2001) passing northward to laterites (Gourdon-Platel et al., 2000). Southward thick deep-water deposits infilled the foredeep. They are made up of gravity carbonate deposits for the Danian and siliciclastic deep-sea-fans for the Thanetian (Dubarry, 1988).
- After a major Early Ypresian retrogradation and a maximum marine flooding of Middle Ypresian age, the *Upper Ypresian* to *Early Lutetian* (*52-44* Ma) time interval corresponds

to a sharp deltaic progradation (Cavelier et al., 1997) driven by an increase in siliciclastic sediment supply coeval with the Pyrenean shortening (Serrano, 2001; Serrano et al., 2001).

- The *Late Lutetian* to *Oligocene* (*44-23* Ma) was characterized by carbonate platforms passing upstream to an alternation of evaporitic lagoonal (clays with gypsum) to continental (lacustrine carbonate, fine-grained fluvial deposits) environments, called 'Molasse' by French authors. This time range is the end of the infilling of the foredeep and the beginning of the propagation of the thrusts in the Aquitaine Basin along the Triassic salt decollement level and the growth of active ridges. The timing of this change of deformation pattern (end of the foredeep and beginning of the thrusting) is poorly constrained. The sediment thickness maps of Serrano (2001) provide age constrains for the end of the foredeep subsidence and the initiation of the propagation of the thrusts in the Aquitaine Basin with the growth of the Audignon thrust and salt ridge (Fig. 1): after a transition period (Nousse Fm, here dated as Lutetian in age, 47.8-43.5 Ma), the growth of the Audignon ridge was active just after the Nousse Fm (here dated of Late Lutetian age, 43.5 Ma). Rocher et al. (2000) measured the shortening of the Landes-de-Siougos Anticline located in the Tartas Subbasin in front of the Audignon thrust (Figs. 1 and 2) that reached a shortening paroxysm during Priabonian times (38-34 Ma).

- The *Early Miocene* (*23-16* Ma) was characterized by marine flooding (the so-called 'Faluns' by French authors) of a large embayment located in the central part of the Aquitaine Basin passing eastward (below the present-day Ger and Lannemezan plateaus) to continental environments dominated by lacustrine limestones (Crouzel, 1957; Antoine et al., 1997). Rocher et al. (2000) measured paleostress magnitudes from calcite twin data in the Arzacq and Tartas Subbasins and suggested a late NW-SE shortening in the Mio-Pliocene.
- The *Middle Miocene* to *Present-Day* (*16-0* Ma) corresponds to the major continentalization of the Aquitaine Basin with the deposition of thin (10-40 m) coarse-grained alluvial deposits (Middle Miocene, 16-11.5 Ma) flooded by the sea during the Langhian and base Serravallian (Gardere et al., 2002; Gardere, 2005). The Pliocene is characterized by sandy alluvial deposits (maximum thickness of 100 m) interstratified with several lacustrine (clays) and marsh (lignites) sediments (Dubreuilh et al., 1995). During the Calabrian (1.8-0.8 Ma) the drainage of the Aquitaine Basin is reorganized from rivers flowing to the Parentis Subbasin to the modern one with a single river conduit, the Garonne-Gironde system (Dubreuilh et al., 1995).

3. Available data and methods

265 *3.1. Available data (Fig. 2)*

266

267 The Aquitaine Basin has been extensively studied since discovery of gas (Lacq structure) in
268 the 1950s (Biteau et al., 2006). Around 40 000 km of seismic reflection lines and 1 600
269 industrial wells were available for this study. In order to date the sediments we focused on
270 some key wells, offshore, Ibis 2 and Pingouin 1 wells (cuttings), onshore Laborde 1D
271 (cuttings) and Landes-de-Siougos (cores) wells (see Fig. 2 for location). We also used the
272 water and geotechnical shallow drillings collected by the French geological survey (BRGM)
273 available in the French drillings database (BSS).

274 In the deep Bay of Biscay and Landes Plateau 35 000 km of industrial and regional seismic
275 lines shot as part of the MARCONI Spanish project, were studied. The only deep wells drilled
276 in that area are DSDP wells (sites 118 and 119 – leg 12 and some leg 48 sites – see Fig. 2 for
277 location), located on top of sea mounts or inverted tilted blocks that make them difficult to
278 use for calibrating the seismic lines of the Bay of Biscay in terms of lithology and ages.

279

280 *3.2. Seismic and wells interpretation: sequence stratigraphy*

281

We here performed a seismic stratigraphic analysis in order to define depositional sequencesTwo approaches of seismic stratigraphy, standardized by Catuneanu et al. (2009), were applied.

The first approach (Brown and Fisher, 1977; Mitchum et al., 1977) is based on the analysis of *seismic reflectors terminations* (onlap, downlap, toplap, truncations). The second one (Helland-Hansen and Gjelberg, 1994; Helland-Hansen and Martinsen, 1996; Helland-Hansen and Hampson, 2009) is based on the *offlap break* (shoreline or shelf-edge break) *trajectory* over time by defining stratal patterns: forced (descending) regressive, normal (ascending) regressive and transgressive.

A depositional sequence is defined here as follows (see Ponte et al. 2019 for a summuary of the different approaches):

- the *sequence boundary*, whichcorresponds to the first correlative conformity (CC, Catuneanu et al., 2009) and the onset in continental domain to the subaerial unconformity, an erosion surface overlain by onlapping strata;
- the forced regressive (FR) deposits (Catuneanu et al., 2009) (equivalent of the forced regressive wedge system tract of Hunt and Tucker (1992) or the falling-stage system tract (FSST) of Plint and Nummedal, 2000), which correspond to descending regressive shorelines (i.e forced progradation) passing toward the deep-sea plain to the basin floor fan;

- the lowstand normal regressive (LNR) deposits (Catuneanu et al., 2009) which correspond to the lowstand system tract (LST) of Posamentier and Vail (1988) or the ascending regressive shorelines (i.e progradation-aggradation) of Helland-Hansen (e.g. Helland-Hansen and Hampson, 2009);
- the *maximum regressive surface* (MRS), which corresponds to the former transgressive or flooding surface Posamentier and Vail (1988) above the toplapping strata;
- the transgressive deposits (T; Catuneanu et al., 2009) which correspond to the transgressive system tract (TST) of Posamentier and Vail (1988) or transgressive shorelines (i.e retrogradation) of Helland-Hansen and Hampson, (2009);
- the *maximum flooding surface* (MFS) which lies below downlapping strata;
- the highstand normal regressive (HNR) deposits (Catuneanu et al., 2009) which correspond to the highstand system tract (HST) of Posamentier and Vail (1988) or ascending regressive shorelines (i.e progradation-aggradation) of Helland-Hansen and Hampson (2009).

Depending on their cause - (eustasy or lithosphere deformation), several orders of depositional sequences of different durations have shaped the past geological periods (Graciansky et al., 1998). As a consequence, the stratigraphic record is a stacking of different orders of nested sequences. Vail et al. (1977) and Vail et al. (1991) defined the orders of

sequences based on their duration: first order sequences have a duration around 100 - 200 Myrs, second order sequences around several 10 Myrs, third order sequences around several 1 Myrs, fourth order around several 100 kys. Determining the hierarchy of depositional sequences (between two sequence boundaries) or stratigraphic cycles (between two MFS) supposed to date the sequences for establishing their order, and possibly their causes.

The nature of the control of the depositional sequences – eustasy or tectonic (lithosphere deformation) is based on (1) the accommodation space measurement using the shoreline wedges on both sides of the sequence boundaries (SB) and (2) the geometrical relationships between the SB and underlying sediments based on the principles (e.g. Robin et al., 1998) that (i) *eustasy* is only a function of space and must have an equal sea level variation value (for a given time interval) over the whole basin and (ii) a *lithosphere deformation* is a function of both space and time, i.e. it may change in amplitude along the basin with possible truncations of tectonic structures with different wavelengths.

The accommodation space is the vertical displacement of the shoreline (Jervey, 1988) and is measured as the vertical displacement of the last shoreline below the SB and the first one preserved above. This distance measured in travel double times are later converted in depth (m) using the velocity law presented in the supplementary materials. Sediment

338 decompactions was not performed: the measurements are therefore the minimum relative
339 sea level variations values.

340 The eustatic curves used are Haq's curve (Haq et al., 1987, 1988; Hardenbol et al., 1998)
341 based on a compilation of coastal onlap curves in different basins of the world and Miller's
342 one (Miller et al., 2005, 2008) based on the accommodation space measurement along the
343 well-known New Jersey margin (New York). The amplitudes of both curves are different and
344 recent studies or compilations (e.g. Bessin et al., 2017 for a review) suggest that the
345 amplitudes measured by Miller's group are more realistic.

346

347

348 Some well-logs correlations using the principles of sequence stratigraphy (Posamentier
349 et al., 1988) and the 'stacking pattern' technique (see van Wagoner et al., 1990; Catunenau,
350 2006) were used for this work.

351

352 A space-time stratigraphic diagram (known as a Wheeler diagram) was compiled (see Fig.
353 8 and supplementary materials) based on the age model (see 3.3), and indicating (1) the
354 amount of time preserved as volumes of sediment, as condensation (no deposition by
355 downlap or onlap) and as eroded sediments or by-pass, (2) the location and nature of the

offlap break (see 3.4), (3) some remarkable environments (alluvial fans and braided alluvial plains) and (4) the lithostratigraphy.

3.3. Sediment dating

The applied dating is a combination of biostratigraphy, orbitostratigraphy and sequence stratigraphy in order to define a high-resolution (0.1 Ma) age model for the Aquitaine Basin both onshore and offshore. This method is developed in supplementary material 1.

The used lithostratigraphic nomenclature is taken from Sztrákos et al. (1997, 1998) and Serrano et al. (2001) for the Eocene, from Sztrákos and Steurbaut (2017) for the Oligocene, of Cahuzac (1980) for the Lower and Middle Miocene and from Dubreuih et al. (1995) from the Upper Miocene to the present-day.

3.4. Reconstruction of the depositional profile

For a given time interval, the reconstruction of successive depositional profiles is based on the lateral evolution of the sedimentary environments from the most proximal preserved continental facies to the deepest marine deposits located on the oceanic crust. Specific attention was paid to the continental environments, major constrain for the reconstruction and the evolution of the sediment routing systems. The characterization of the sedimentary

environments is based on (i) the facies sedimentology of the cores and outcrops, (ii) the palaeoecology provided by the faunas and floras fossilized in the cuttings and (iii) the seismic geometries.

The location of the *shoreline* is based on the identification of offlap breaks. There are at least two types of offlap breaks (1) shorelines or (2) shelf breaks (e.g. Helland-Hansen and Hampson, 2009). They also can result from subaqueous shoals or reef breaks in carbonate platforms. In order to discern shorelines from shelf breaks a well control is required to check, in the case of shorelines, that upstream facies are clearly continental, based on the lithology (e.g. coal) and palaeoecology provided by the cuttings or the well-logs signatures (see van Wagoner et al., 1990; Catuneanu, 2006).

The reconstruction of the *marine environments* is based on a seismic analysis of the clinoforms and certain specific seismic geometries. In marine environments, the high and slope of the clinoforms provide indications regarding their origin (delta front, slope downstream of the shelfbreak – see Patruno and Helland-Hansen, 2018, for a review). We did not study deep-sea deposits, e.g.deep-sea fans, contouritic ridges, sand-waves as it was outside the scope of this study.

394 *3.5. Isopach maps*

395

396 Two isopach maps were built in this study based on the seismic interpretation of the
397 available seismic lines, a first one from the Palaeocene to Oligocene (66-23 Ma) and a
398 second one from the Miocene to today (23-0 Ma).

399 The base Palaeocene (base Cenozoic) and base Miocene (base Neogene), as well as other
400 key surfaces, were propagated from the present-day Pyrenean piedmont to the distal part of
401 the Bay of Biscay using the sequence stratigraphy principles, based on seismic lines (90% of
402 the area), shallow wells (BSS database) and 1:50 000 geological maps at for the onshore
403 outcropping areas. The main concern was the conversion of seismic lines from two-way
404 travel time (TWT) in seconds into depth in meters, using velocity laws (see supplementary
405 materials) available from the industrial wells that were compiled as part of this study. The
406 extrapolation of the 2D (seismic lines) and 1D (wells) data, both irregularly distributed, was
407 based on the Natural Neighbour method (GIS).

408

409

410 **4. Results**

411

412 *4.1. Main steps of the Aquitaine Basin infilling: sequence stratigraphy*

413

414 *4.1.1. Main sedimentary environments*

415

416 The *continental environments* of the Aquitaine Basin can be grouped into three facies
417 associations characteristic of different depositional profiles and slopes: (1) extensive
418 lacustrine to palustrine facies alternating with fluvial systems, (2) megafans or braided
419 alluvial plains and (3) alluvial fans.

420 • The *lacustrine to palustrine* environments – which can be correlated over a distance of
421 several tens of kilometers up to one hundred kilometers – that alternate with *fluvial*
422 *channels* (*alluvial* to *coastal plains*) indicate nearly flat domains with almost no slope. For
423 large coastal plains, the cuttings and cores contain dinocysts (e.g. Mudie et al., 2017) and
424 no marine microfaunas (absence of benthic foraminifers and calcareous nannofossils).
425 The lithology is either claystones with evaporites (gypsum) in the case of evaporitic
426 coastal plains (e.g. Warren, 2010) or claystones with coals (lignites) in the case of
427 marshes (palustrine environments – McCabe, 1984). For extensive lakes (e.g. Gierlowski-
428 Kordesch, 2010), the cuttings and cores are made up of correlatable micritic to bioclastic
429 limestones with charophytes (e.g. Anadon et al., 2002) and fresh water gastropods
430 (limnees, planorbes, etc). The interstratified channels are composed of medium to fine-

grained sandstones without any marine fossils. They correspond to suspended-load to mixed-load fluvial channels.

- The *megafans* to *braided alluvial plains* are homolithic coarse-grained sandy (sometimes with pebbles) deposits continuous over a distance of several tens to one hundred of kilometers, without any marine fossil (Singh et al., 1993; Shukla et al., 2001). They correspond to a stacking of bedload fluvial channels. The main difference between megafans and braided alluvial plains is the source of sediments deduced from palaeogeographic maps: point source for the megafans and multiple sources for the alluvial braided plains.
- The *alluvial fans* are mostly homolithic conglomerates continuous over a distance of several kilometers to ten kilometers, without any marine fossils (e.g. Stanistreet and McCarthy, 1993; Blair and McPherson, 2009), with some evidences of ephemeral lakes (non correlatable "multi-coloured" clays) or subaqueous soils (calcretes s.l.).

The *shallow marine environments* of the Aquitaine Basin are mainly mixed siliciclastic – carbonate platforms. They became siliciclastic - similar to the modern environments, in Middle Miocene. Previously based on the seismic geometries or on facies on cores, there are two types of depositional profiles (i) rimmed carbonate platforms or (ii) ramps (e.g. Handford and Loucks, 1993). Rimmed carbonate platforms – the most common profile – are

450 highly variable. The barrier may be large reefal build-ups, reef patches or bioclastic shoals. At
451 the back of these barriers, the inner platform may be (i) more or less large lagoons or bays
452 passing upstream to the above described coastal plain or (2) large tide-dominated epeiric
453 seas (called the 'faluns' by French authors).
454
455 *4.1.2. Description: second order sequences*
456 In the Aquitaine Basin major sequences boundaries (SB) are defined using three criteria:
457 (1) a removal of at least several tens of meters of accommodation space, (2) a change in the
458 sedimentary system and/or (3) the importance of erosional truncations of the underlying
459 sediments. They may be distributed in the Aquitaine stratigraphic record as single SB or as
460 sets of several SB due to a long term (second order) decrease or removal of the
461 accommodation space upon which the shorter (third order) accommodation variations were
462 superimposed. In this second case the base of the second order sequence is defined here as
463 the first SB.
464
465 Four unconformity-bounded second order sequences were identified along the Aquitaine
466 platform, from the uppermost Ypresian until today.
467
468 *YP's second order sequence (Late Ypresian - lowermost Priabonian – 49.7-37.6 Ma)*

The *age* of the base sequence boundary (SByp) is Late Ypresian (49.7 Ma - base of the Lussagnet Fm – see supplementary material 1 for age constrains). The age of the MFS (YP-MFS-4) is at the base of the Bartonian (41.6 Ma – within the lower member of the Brassempouy Fm). At least five main third order sequences were identified.

The *base sequence boundary* (Fig. 5 and supplementary material 2) separates a highstand normal regressive (HNR) wedge (possible pure progradation) from a lowstand normal regressive (LNR) wedge with no forced regressive deposits in between. The amplitude of the relative sea level of fall is 40 to 80 ms, i.e. 51 to 104 m (velocity law: 2540 to 2590 m/s). No tectonic structures are truncated by this sequence boundary (Figs. 3 and 6).

The YP sequence is characterized by downlap terminations, with time condensation in the deepest part of the Aquitaine platform (Fig. 8).

The *depositional profile* changed trough times with three main periods.

- The Late Ypresian depositional profile (Table 1) is characterized onshore by megafans deposits (Lussagnet Fm) mainly fed from the French Massif Central (Schoeffler, 1971) supplying a large deltaic system (Donzacq Fm , E. lasseur and J. Briais, work in progress).
- The Early Lutetian and Late Lutetian depositional profiles (Table 1) are very similar starting with an alluvial fan (Member 1 of the Palassou Fm - eroded during Chattian times along section LR6 - Fig. 3) passing to nearly flat alluvial to coastal plains (Cavalante Fm and Tartas Fm). The main difference concerns the carbonate platforms that are both

reef rimmed carbonate platforms and flat (Nousse Fm) for the Early Lutetian and with seismic-scale build-ups (Brassempouy Fm) for the Late Lutetian/Priabonian.

PC's Second order sequence (lowermost Priabonian – Chattian – 37.6-27.1 Ma)

The *age* of the base sequence boundary (SBpc) is at the base of the Priabonian (37.6 Ma - base of the Campagne Fm, just above the top of the Brassempouy Fm – see supplementary material 1 for age constrains). The age of the MFS (PC-MFS-9) is Late Rupelian (29.4 Ma – base of the upper member of the Mugron Fm). At least five main third order sequences were identified.

The *base sequence boundary* (Figs. 4 and 5, supplementary material 2) separates highstand normal regressive (HNR) wedge from a lowstand normal regressive (LNR) wedge with no forced regressive deposits in between. The amplitude of the relative sea level of fall is difficult to quantify due to the poor offlap break record and doubts regarding their nature (shorelines or shoal highs). It ranges between 40 ms and 90-80 ms, i.e. 52 to 123 m (velocity law: 2580 to 2620 m/s). No tectonic structures of any wavelength are truncated by this sequence boundary. Along the Mirande Subbasin (Fig. 3) the depocenters migrated northward of the salt-controlled faulted anticlines (St-Medard, Auch).

The third order sequence boundaries show a well-recorded forced regressive (FR) wedge for the intra-Priabonian (PC-SB-7) one and no forced regressive wedge but with a marked

onlap for the uppermost Priabonian (PC-SB-8) one. The amplitude of the intra-Priabonian relative sea level fall is 150 ms, i.e. 188 to 191 m (velocity law: 2500-2550 m/s) and the amplitude of the uppermost Priabonian is 60 ms (minimum estimation) i.e. 74 to 75 m (velocity law: 2470-2500 m/s).

The Priabonian to Rupelian *depositional profile* (Table 1) is very similar to the Lutetian profiles, with upstream alluvial fans (member 2 and 3 of the Palassou Fm and its westward equivalent, the Jurançon Fm – Fig. 3 and 8) with, as a local base level, nearly flat alluvial to coastal plains (Campagne and Agenais Fms). The carbonate platforms are made up of bio-constructed mounds (or shoals – Siest Fm - Priabonian) or patchy reefs along a mixed siliciclastic-carbonate ramp (Gaas and Mugron Fms – Rupelian).

CT's Second order sequence (Chattian-base Tortonian – 27.1-10.6 Ma)

The *age* of the base sequence boundary (SBct) is Early Chattian (27.1 Ma - top of the Mugron Fm or base of the Escornebéou Fm – see supplementary material 1 for age constrains). The age of the MFS (CT-MFS-15) is Late Burdigalian (17.5 Ma – intra Pontonx Fm). At least eight main third order sequences were identified.

The *base sequence boundary* is topped by a stacking of third order sequences organized in a large second order forced regression (FR) wedge, comprising at least two third order sequence boundaries (CT-SB-12a – 26.4 Ma and CT-SB-12b – 25.2 Ma). The amplitude of the

relative sea level fall is difficult to estimate, once again due to the nature of the offlap break (shoreline or shelfbreak). The maximum value from the shoreline (upward offlap break) to a possible shelfbreak (downward offlap break) is 160 ms, i.e. 192 to 198 m (velocity law: 2400-2470 m/s). The water depth of the shelfbreak can be deduced from the height of the shelf clinoforms (topped by the shoreline), i.e. 60 to 62 meters (50 ms). The relative sea level fall is therefore around 132 to 136 m. Along the Northern Pyrenean Front (line LR6, Fig. 3 and 'offshore-shore-parallel' line, Fig. 6), the structures (North-Pyrenean Front, downstream thrusts and folds and salt-related anticlines – e.g. St-Médard, Auch, Landes High diapirs, etc.) are truncated by the latest Chattian SB (CT-SB-12b – 25.2 Ma).

The Chattian to base Tortonian *depositional profiles* (Table 1) changed over time. Their common characteristic is the occurrence of large marine embayments, corresponding to mixed bioclastic-siliciclastic tide-dominated deposits ('faluns' as per French authors).

- Onshore the Early Miocene depositional profile (Table 1) is a large coastal to nearly flat alluvial plains with carbonate lacustrine deposits ('Calcaires blancs de l'Agenais' Fm) onlapping the SB southward (Crouzel, 1957 – Fig. 8).
- The Middle Miocene depositional profile (Table 1) is characterized onshore by braided alluvial deposits ('Sables fauves' Fm - Gardere et al., 2002; Gardere, 2005) passing upstream to alluvial fans. These fans are located downstream from the pre-Chattian ones, south of the North Pyrenean Front thrusted between these two generations of

fans (Fig. 8). Carbonate lakes (e.g. Auch and Astarac Fms) occurred in between or in front of these alluvial fans (Crouzel, 1957).

The major environmental change of the 'Sables fauves' Fm corresponds to a significant third order SB (CT-SB-16, 16.4 Ma), followed during uppermost Langhian times (CT-SB-17, 14.7 Ma) by a second one coeval with the fluvial valley incisions (Gardere et al., 2002; Gardere, 2005).

The two offshore canyons (Fig. 1) are initiated (Cap Breton Canyon) or became active (Cap Ferret Canyon) just after the last Chattian SB (CT-SB-12b, 12.5 Ma, i.e. at the end of the forced regressive wedge (Fig. 6 and 7) feeding the so-called Cap Ferret deep-sea fan.

TT's Second order sequence (base Tortonian-today – 10.6-0 Ma)

The *age* of the base sequence boundary is well dated onshore at 10.6 Ma (base of the 'Argiles à galets' Fm at the boundary with the Montréjeau ('Molasse') Fm – see supplementary material 1 for age constraints). Only the first progradational trend of the sequence is preserved. At least six main third order sequences were identified.

The *base sequence boundary* (SBtt) is onshore (Fig. 3) an aerial unconformity and offshore (Fig. 5) a SB topped by a lowstand normal regressive (LNR) wedge. The uncertain nature of the offlap break (reasonably the shelf break) means that no relative sea level measurements can be taken.

564 The base Tortonian to today *depositional profiles* (Tab. 1) changed over time. They are
565 characterized onshore by (i) low sediment preservation or aerial erosion and (ii) by a coastal
566 plain corresponding to the present-day Landes Forest and offshore by pure siliciclastic shelf
567 deposits. Along the alluvial plain the Tortonian to Early Pleistocene times correspond to the
568 growth of low preservation megafans (pebbly coarse-grained sands of the 'Argiles à galets'
569 Fm) with numerous evidences of by-pass periods (Fig. 8). The coastal plain (see 2.3) is a
570 stacking of low preservation fluvial sediments (coarse to medium-grained sands) and
571 marshes deposits (lignites). Although poorly dated, the Early to Middle Pleistocene is a
572 period of major incision of the alluvial systems with numerous incised valleys (Dubreuilh et
573 al., 1995).
574
575 *4.1.3. Interpretation: tectonic or eustatic controls of the second order sequences*
576
577 The *second order sequence boundary (SByp) of Late Ypresian age* (49.7 Ma - base of the
578 Lussagnet Fm) recorded (1) a relative sea level fall of 50 to 105 m, (2) no deformations with a
579 wavelength shorter than the size of the Aquitaine Basin and (3) a major change in the
580 sediment routing system with the brief growth of a megafan (Lussagnet Fm, Fig. 8).
581 According to Haq et al. (1987, 1988), the end Ypresian is characterized by a major short
582 eustatic fall (130-140 m), whereas Miller et al. (2005, 2008) quantified a quite minor one

around 40 m. Haq's value is too high compared to what was measured here and is therefore questionable (see the comments on Haq's curve in 3.1). The Miller's accommodation measurements provide a maximum value for this eustatic fall. Our values are higher than 40 m and therefore a tectonically-enhanced eustatic fall in response to basin-scale deformations is the most reasonable explanation for this unconformity. This is supported by the short perturbation (in time) of the sediment routing system with the growth of megafans.

The *second order sequence boundary (SBpc) of the base of the Priabonian* (37.6 Ma - base of the Campagne Fm) recorded (1) a relative sea level fall of 50 to 125 m and (2) a reorganization of the subsiding areas. Haq's studies (1987, 1988) indicate a major eustatic sea level fall of around 90 m, when Miller's work confirmed a major one of 70-80 m. This last value falls with in the range of our measurements and therefore a eustatic origin may be inferred for this sequence boundary (SBpc). Nevertheless, the reorganization of the subsidence pattern and relative sea level variations ranging up to 125 m, may once again suggest tectonic forcing.

The *third order sequence boundaries of intra-Priabonian* age (PC-SB-7) recorded a relative sea level fall of 190 m. This value is much higher than the eustatic variations of 30-40 m proposed by Haq (1987) and a tectonic origin is proposed here.

601 The *third order sequence boundaries of uppermost Priabonian* age (PC-SB-8) recorded a
602 relative sea level fall of 75 m. In terms of age, this event occurred before the major sea level
603 fall of the Eocene-Oligocene boundary of around 100 m (Miller et al., 2008) due to the onset
604 of the Antarctic glaciation (transition to icehouse conditions). A tectonic origin is therefore
605 proposed for this SB.

606 The *second order sequence boundary (SBct) of Early Chattian* age (27.1 Ma - top of the
607 Mugron Fm or base of the Escornebéou Fm) recorded (1) a relative sea level fall of 190 to
608 200 m and (2) the late deformation stages of the North Pyrenean Front and related tectonic
609 structures which are no longer active beyond 25.2 Ma. This second point indicates a tectonic
610 control of this sequence boundary confirmed by the amplitude of the relative sea level fall
611 (190-200m) which is much higher than the eustatic variations occurring during Chattian
612 times (around 30 m for Haq and around 40 m for Miller). The truncation of all of the
613 structures, both major (North Pyrenean Front) and minor (salt-controlled thrusts and folds)
614 by the third Chattian SB (CT-SB-12b, 25.2 Ma) support a very long deformation period
615 initiated at the base of the forced regression wedge (SBct) i.e. from 27.1 Ma to 25.2 Ma.

616 The *second order sequence boundary (SBtt) of base Tortonian* age (10.6 Ma - base of the
617 "Argiles à galets" Fm is much younger than the major eustatic fall of Late Serravallian age
618 due to an increase in the volume of the Antarctic ice sheet (Zachos et al., 2001; Miller et al.,
619 2011); therefore, a tectonic origin can be assumed even though it was not possible to take

any measurements of the relative sea level fall here. The SBtt probably records the paroxysm of a period of uplift (see 5.1) initiated during the uppermost Burdigalian (CT-SB-16, 16.4 Ma) at the time of the onset of the braided alluvial plain deposits of the 'Sables Fauves' Fm.

4.2. Sediment distribution through space and time: isopach maps

4.2.1. Description (Figs. 9 and 10)

The *Palaeocene* to *Oligocene* (*66-23* Ma – up to CTf7) isopach map (Fig. 9) shows a clear difference between the Aquitaine Basin and the Bay of Biscay deep basin with a low accumulation zone in between corresponding to the Landes Plateau offshore and the Landes High onshore. In the Bay of Biscay deep basin, two main depocentres can be defined; (i) a first one located north of the Le Danois Bank (up to 2500 m of sediments in 23 Ma) with few sediments eastward toward the present-day Cap Ferret Canyon and (ii) a second one located in the Armorican Subbasin northwest of the Gascogne Dome (up to 2000 m in 23 Ma). A little patch of sediment is preserved in front of the present-day Cap Ferret Canyon. Seismic data suggest a Late Eocene to Oligocene age for this patch. In the Aquitaine Basin/Landes Plateau area two main domains can be defined according to the Pamplona Transfer Zone

639 and its poorly known possible northward prolongation toward the Aquitaine Basin.
640 Westward toward the Landes Plateau, three units can be recognized, from south to north, (i)
641 a major depocenter (up to 3500 m of sediments in 23 Ma) located south of the Cap Breton
642 Canyon, (ii) a low accumulation zone corresponding to the Landes Plateau and Landes High
643 and (iii) a medium accumulation zone (up to 2500 m in 23 Ma) around and north of the
644 Parentis Basin. Eastward along the present-day onshore Aquitaine Basin patchy main
645 depocentres occurred in the Arzacq, Tarbes and Carcassonne Subbasins. Low sediment
646 accumulations characterized the Audignon and Maubourguet Ridges. The amount of
647 sedimentation is very low north of the Aquitaine Basin, along a line that more or less
648 corresponds to the Celtaquitaine 'flexure', the former onlap of the Triassic salt deposits. In
649 between the two domains (Landes Plateau and High and present-day onshore Aquitaine
650 Basin) a north-south trending depocentre crossed the Thétieu Fault along the possible
651 prolongation of the Pamplona Fracture Zone.
652
653 The *Miocene* to *today* (*23-0* Ma – from CTf7) isopach map (Fig. 10) again shows a major
654 difference between the Aquitaine Basin and the Bay of Biscay deep basin. In the Bay of
655 Biscay deep basin, a single depocentre (up to 3000 m in 23 Ma) is located at the intersection
656 between the mouths of the present-day Cap Ferret Canyon eastward and Torrelavega and
657 Santander Canyons southward. This depocenter extends as an east-west ribbon bounded by

658 two low sediment accumulations domains, the Gascogne Dome to the north and the
659 Cantabria Mountains to the west. In the Aquitaine Basin/Landes Plateau area two main
660 domains can be defined according to the Pamplona Transfer Zone and the Thétieu Fault.
661 Westward the Landes Plateau is made up of several patches of depositional and very low
662 depositional zones with sediment accumulations (up to 2000 m in 23 Ma) along (i) the
663 Cantabrian Margin, (ii) the axis of the Cap Breton Canyon, (iii) the Parentis Basin and (iv) the
664 axis of the Cap Ferret Canyon. A low sediment accumulation axis is located north of the front
665 the Basque-Cantabrian Basin. The south-eastern part of the South Armorican shelf was a low
666 accumulation area forming a southward thickening wedge of sediments. The present-day
667 onshore Aquitaine Basin was a quite low sediment accumulation domain (20 to 500 m in 23
668 Ma) with three main depocentres: (i) a wedge at the transition with the Landes Plateau in
669 the continuity with the one of the South Armorican Shelf, (ii) in the Tartas Subbasin north of
670 the Audignon Ridge and (iii) in the Tarbes Subbasin (up to 200 m in 23 Ma).
671
672 *4.2.2. Interpretation : sink preservation and lithosphere deformation*
673
674 From *Palaeocene* to *Oligocene* (*66-23* Ma) times, the sediment thick accumulations
675 located at the front of the Pyrenees and Basque-Cantabrian folds and thrusts belts
676 correspond to foredeeps, i.e. the north Basque-Cantabrian, Arzacq, Tarbes and Carcassonne

depocenters. The occurrence of three north Pyrenean foredeeps (Arzacq, Tarbes and Carcassonne) and the major role of the Pamplona Transfer Zone suggest a strong segmentation of the foreland basin in good agreement with the numerical modelling of Angrand et al. (2018) taking the Albian rifting inheritances into account. The meaning of the Basque Cantabrian depocenter is debatable: does it represent the western end of the South Pyrenean pro-foreland Basin or the merging of both forelands, i.e. the pro- and retro-forelands? The palaeocurrent pattern (towards the S-SW) of the Jaizkibel Ypresian turbidites (Kruit et al., 1972) located east of the Basques Massif (Fig. 9), may support this second scenario with the deflection of the turbidity currents coming from the Arzacq foredeep along the emerged Basques Massif, in good agreement with the palaeogeographic reconstructions of Vacherat et al. (2017).

During Cenozoic times, the Landes High behaved as a rigid zone perturbing the flexural response of the lithosphere due to mountain loading.

At shorter wavelengths, salt-related thrusts and associated anticlines or ridges (Audignon, Maubourguet) started to be active, in good agreement with the Lutetian age of the onset of these structures (Serrano, 2001 – see 2.3).

In the Bay of Biscay deep basin, the Santander transfer zone is active controlling the limit between accumulating and non-accumulating domains. The deposits forming the patch of sediments located northward of the transfer zone and westward of the present-day Cap

696 Ferret Canyon may be fed either by a proto-Cap Ferret Canyon or by proto-Torrelavega-
697 Santander Canyons during Late Palaeogene times. The depocentre located north of the Le
698 Danois Bank is interpreted here as the products of the erosion of the inverted Asturian Basin
699 (Le Danois Bank) during the Late Eocene to Oligocene (Gallastegui et al., 2002). The
700 depocenter of the Armorican Subbasin is controlled by the inversion of the lower Cretaceous
701 extensional blocks during Palaeocene and Upper Eocene times (Thinon, 1999; Thinon et al.,
702 2001, 2002) and fed by rivers coming from the uplifted Armorican Massif (Guillocheau et al.,
703 2003).
704
705 From *Miocene* to *today* (*23-0* Ma) times, the thick sediment accumulation zones located
706 in front of the Pyrenean Belt during the previous time interval no longer existed, confirming
707 the end of the foredeep before 23 Ma (during the Lutetian, according to Serrano, 2001).
708 Nevertheless, some salt-controlled blind thrusts (Audignon Ridge) are still controlling a low
709 differential subsidence between the Arzacq and Tartas Subbasins (Fig. 9), which is discussed
710 later (5.2.1). The contour lines of the Tarbes Subbasin may be partly residual due to the
711 erosion and growth of the Lannemezan Plateau in Tortonian times (SBtt - see 4.1).
712 In the Bay of Biscay deep basin, the main depocentres corresponds to a major deep-sea
713 fan fed by both the Cap Ferret Canyon and the Torrelavega and Santander Canyons the last
714 canyon is supplied by the Cap Breton Canyon (initiated at the end of the Chattian, post CT-

SB-12b, i.e. post 25.2 Ma). The inverted structures of the Gascogne Dome and its westward prolongation (Thinon, 1999, Thinon et al., 2001, 2002) have controlled the location of the deep-sea fan. At that time, the Cantabrian Seamount is a submarine relief.

4.3. First order evolution of the sediment preservation during Cenozoic times: a regional 2D section

4.3.1. Description (Fig. 11)

A regional E-W seismic line (Fig. 11) has been compiled from the onshore Aquitaine Basin, north of the Lannemezan Plateau, to the Bay of Biscay deep basin. This section crosses the Aquitaine platform north of the foredeep, the Landes Plateau and the Torrelavega-Santander Canyons and reaches the deep-sea abyssal plain of the Biscay Basin.

At the first order the *Aquitaine platform* was progradingng from Ypresian times (Serrano et al., 2001) with 1400 to 700 m high clinoforms. This section confirmed (see 4.2) the specific nature of the *Landes Plateau* that behaved as a quite low accumulation zone during the Cenozoic. From the offshore Aquitaine Basin to the Landes Plateau, several pre-existing salt diapirs of Cretaceous age were reactivated during Cenozoic times. The *Bay of Biscay deep-sea plain* – not studied in details here – is composed of deep-sea fans and oceanic

currents deposits (contouritic mounds and ridges, sand-waves). The deep-sea fans initiated during the end of the Palaeogene and active since the last Chattian SB (CT-SB-12b, 25.2 Ma), are characterized by few channel deposits (rare occurrences on strike seismic lines) and are mainly made up of stacked turbiditic lobes. Oceanic currents deposits were preserved from the Late Chattian and became dominant along the slope from Messinian times.

This section can be subdivided into three main units bounded by major discontinuities that correspond, in the continental record, to the subaerial unconformities (sequences boundaries) of Chattian (27.1-25.2 Ma) and Early Tortonian (10.6 Ma) age (4.1) (see captions in Fig. 11 for an age discussion).

- From *base Cenozoic to Chattian* times (66 to 27.1-25.2 Ma), most of the sediments were stored in the Aquitaine platform with some in the Bay of Biscay deep-sea plain. At the first order, the progradational wedge was mixed progradational-aggradational. The offlap break was the shoreline. The clinoforms (slope: 1 to 1.5°; height up to 1400 m) correspond to mixed carbonate-siliciclastic slopes to ramps and during the Late Ypresian to deltas. The map of the Palaeogene sediment thickness (Fig. 9) suggests that the sediments of the Bay of Biscay deep-sea plain were fed from the inverted and eroded Asturian Basin (4.2.2). A high preservation on the Aquitaine platform and its consequence, a low export toward the continental slope and the deep-sea plain, are in

753 good agreement with the high amount of condensation by downlap measured during
754 this time interval (see the Wheeler diagram, Fig. 8).

755 • From *Chattian to Early Tortonian* times (27.1-25.2 to 10.6 Ma), sediments were
756 distributed all along the depositional profile, with less sediment on the platform than in
757 the deep-sea basin. At the first order, the progradational wedge while progradational-
758 aggradational, was dominated by the progradation. The offlap break was either the
759 shoreline or shelf break. The clinoforms (slope: 1.5 to 2°; height: 1200-1400 m)
760 correspond to mixed carbonate-siliciclastic slopes. Since 25.2 Ma both Cap Ferret and
761 Cap Breton Canyons (see Fig. 1 for location) were actively transferring (laterally to the
762 section) sediments toward the Cap Ferret deep-sea fan.

763 • From *Early Tortonian to present-day* times (10.6 to 0 Ma), most of the sediments were
764 stored in the Bay of Biscay deep basin, with a very thin layer of continental sediments
765 preserved on the Aquitaine platform. At the first order, the progradational wedge is a
766 purely progradational one. The offlap break is the shelfbreak. The clinoforms (slope: 2.5
767 to 5.5°; height: 700-1000 m) correspond to siliciclastic slopes.

768

769 *4.3.2. Interpretation*

770

From the base Cenozoic to today, the sediment preservation, i.e. sink preservation, changed through time with a first period when most of the sediments are preserved on the platform, a second one when the sediment distribution is more well-balanced between the platform and the deep basin with a slight imbalance in favour of the deep basin and a third one when most of the sediments are preserved in the deep basin.

The sink preservation evolution observed here may be explained by the balance between the accommodation space created by the subsidence [A_{sub}] and siliciclastic sediment supply [S_{sc}] over tens of million years (Posamentier and Allen, 1993; Catuneanu, 2006). The first order measurement of tectonic subsidence (Desegaulx and Brunet, 1990) indicates an increasing rate from the Palaeocene (maximum rates: 2 to 9 m/Ma) to the Eocene (maximum rates: 21 to 83 m/Ma) and then a decrease until the present day. Many thermochronological studies document the main exhumation phase of the Axial Zone during late Eocene-early Oligocene (Fitzgerald et al., 1999, Gibson et al., 2007, Fillon and van der Beek, 2012, Dinclair et al., 2005) suggesting an increase of the erosion rate and of the siliciclastic sediment volume feeding the basin.

- When $\Delta A_{sub} \leq \Delta S_{sc}$, most of the sediment are preserved on the platform and few siliciclastic sediments are transferred and preserved in the deep-sea plain. The stratigraphic pattern is aggradational ($\Delta A_{sub} = \Delta S_{sc}$) or progradational-aggradational ($\Delta A_{sub} \leq \Delta S_{sc}$ with low differences between ΔA_{sub} and ΔS_{sc}).

- When $\Delta A_{sub} < \Delta S_{sc}$ (with significant differences between ΔA_{sub} and ΔS_{sc}), most of the produced siliciclastic sediment are transferred to the deep-sea plain. Some sediments may be preserved on the platform.
- When $\Delta A_{sub} << \Delta S_{sc}$, most of the produced siliciclastic sediments are crossing through the platform (by-pass to low preservation) and are preserved in the deep-sea plain.

5. Discussion

5.1. Deformation causes sediment routing and sink preservation changes

The Aquitaine Basin recorded at least two wavelengths of deformation: (1) thrusts and anticlines (ridges and domes) related to the Triassic salt decollement level, with a wavelength of several tens to one hundred kilometers (medium wavelength) and (2) at the basin-scale, i.e. with a wavelength of at least several hundreds of kilometers (long wavelength).

5.2.1. Medium wavelength deformations: *salt-related thrust and ridges*

Thrusts and related salt diapirs and anticlines (ridges) were initiated quite early in the retro-foreland evolution during the Lutetian (Serrano, 2001 – see 2.3) with a paroxysm of shortening during the Priabonian (Rocher et al., 2000 – see 2.3) that might correspond to the 35.8 Ma SB (PC-SB-7, intra-Campagne Fm, intra-Priabonian) and the related uplift occurring north of the Audignon Ridge. These deformations are truncated and sealed at 25.2 Ma (CT-SB-12b).

Some seismic lines show evidence along salt-controlled anticlines of pure vertical movements after 25.2 Ma (Fig. 3, e.g. St-Medard Anticline), i.e. after the end of the shortening. Some authors (Rocher et al., 2000 onshore Aquitaine; Ferrer et al., 2012 offshore Aquitaine) interpreted these structures as an indicator of the latest Pyrenean compression. We interpret these structures as a result of differential sediment loading in response to high sediment supply.

*5.2.2. Long to very long wavelength deformation*s

Basin-scaledeformations – mainly regional uplifts - may have occurred during the Late Ypresian (SByp) and occurred during the Chattian (SBct to CT-SB-12b) and Early Tortonian (SBtt).

826 The possible *Late Ypresian* (49.8 Ma) basin-scale uplift may be related to the end of the
827 period of increase of mountain shortening and the incorporation of thicker portions of crust
828 in the collision belt, ranging from the Palaeocene to Early Eocene (Ypresian) as proposed by
829 Mouthereau et al. (2014) and Teixell et al. (2016) (see 2.2 and Fig. 12).

830 The *Chattian* forced regression wedge and its related SB (SBct to CT-SB-12b) record a
831 quite long lasting (27.1-25.2 Ma) basin-scale uplift. The last Chattian SB (CT-SB-12b, 25.2 Ma)
832 eroded and fossilized the North Pyrenean Front and the medium wavelength salt-related
833 thrusts and anticlines, and thus itrecords the end of the compression and then the evolution
834 from the syn-orogenic to post-orogenic period. This is in good agreement with the plate
835 kinematics data (Roest and Srivastava, 1991) indicating a stop of the convergence between
836 Eurasia and Iberia around the Oligocene-Miocene boundary (see 2.2).

837 The origin of the *Early Tortonian* deformations– an uplift with truncations of the Pyrenean
838 piedmont and a stop of the subsidence in the area of the present-day Landes, which is
839 clearly post-orogenic as indicated by the absence of compressive structures truncated by
840 this the Early Tortonian SB (SBtt), is probably at a longer wavelength than the Aquitaine
841 Basin. This unconformity is announced by the facies changes and the SB at the base of the
842 'Sables fauves' Fm deposited in a large braided alluvial plain, of base Langhian age (around
843 16 Ma). In Western Europe, this time interval corresponds to major uplifts (e.g. Ziegler,
844 1990; Ziegler and Dèzes, 2007; Carminati et al., 2009). In the French Massif Central, the

Middle to Late Miocene corresponds to (1) the emplacement of the Cantal strato-volcano at 13 Ma (paroxysm at 7.2 Ma, Nehlig et al., 2001) on top of a mantle anomaly (Granet et al., 1995a,b; Barruol and Granet, 2002) and (2) to the first incision and then uplift of the Upper Tarn (13 Ma, Ambert and Ambert, 1995) and Upper Loire (8.2 Ma, Defive et al., 2007). In the Armorican Massif, the incision of river drainage filled by Late Tortonian to Messinian sediments (Red Sands) recorded a massif-scale uplift (Guillocheau et al., 2003; Brault et al., 2004). In southern Britain (Weald Basin), a major denudation occurred during Mio-Pliocene times in response to a southern Britain-scale uplift (e.g. Jones, 1980). In southern Germany, in the area located between the Rhine Graben and Bohemian Massif north of the Alpine Foreland Basin, geomorphological studies of the stepped planation surfaces and related scarps (Bremer, 1989) indicate a major low amplitude uplift of this area during Miocene times (poorly dated). In conclusion, this brief but not exhaustive review of Western Europe uplifts, suggest a major Western Europe-scale uplift during Middle and Late Miocene times. Because of this very long wavelength (more than 1 000 km), this deformation might be related to mantle dynamics coeval with the Alps formation.

5.2.3 Sink preservation and sediment routing system in the Aquitaine/Bay of Biscay Basins during Cenozoic times.

Two alluvial systems composed the aerial part of the sediment routing system of the Aquitaine Basin (see 4.1.1): (1) a nearly flat fluvial system (suspended-load and mixed channels) with widespread lakes and marshes and (2) alluvial (mega)fans or braided alluvial plains. The alluvial fans may be small to medium sized (several kilometers to several tens of kilometers long from the upstream source to the downstream ultimate deposition – Palassou and Montréjeau 'Molasse' Fms) or large ones (several tens to hundred kilometers- the so-called megafans – Lussagnet Fm). Nearly flat fluvial to lacustrine systems, megafans and large braided alluvial plains ('Sables fauves' and 'Argiles à galets' Fms) are connected to the sea level, while small to medium-size alluvial fans are connected to local base levels corresponding to the nearly flat fluvial to lacustrine systems.

The most intriguing unexpected result is the occurrence of nearly flat alluvial plains in a foreland basin at the feet of growing up mountain belts. This raises the corollary question of the existence of similar flat depositional topographies in other foreland basins. The South Pyrenean pro-foreland basin evolved differently from its twin North Pyrenean (Aquitaine) retro-foreland. One of the major differences is the closure and disconnection of the basin from the sea at the time of uplift of the Basque-Cantabrian Mountains at 37Ma (Gomez et al., 2002). Unfortunately, no or few widespread lacustrine systems have been described during the exoreic phase of the foreland. The Swiss Molassic Basin (Homewood et al., 1986; Berger et al., 2005) began as a deep basin with turbidites filled by deltaic progradations

(Lower Marine Molasse – Rupelian to Early Chattian). They passed upward into fluvial and lakes deposits (Lower Freshwater Molasse – Early Chattian to Early Aquitanian), the local base level of the large alluvial fans active up to the Middle Miocene. After a marine flooding (Upper Marine Molasse – Late Aquitanian to Burdigalian) the basin is filled by lacustrine, fluvial and alluvial fans deposits (Upper Freshwater Molasse – Middle Miocene). This example also indicates the occurrence of lacustrine deposits as well as widespread marine flooding, both suggesting quite low slope alluvial plains for the Swiss Molassic foreland basin. This might suggest that the Aquitaine retro-foreland basin is not a unique case example. Nevertheless, more sedimentological studies focussing on the palaeotopography of alluvial plains are required for other foreland basins.

The Aquitaine retro-foreland basin from 50 to 16.4 Ma suggests an equilibrium between accommodation space and sediment influx : nearly flat fluvial to lacustrine systems behave as a local base level for the alluvial fans. This time span covered both the foreland stage and first post-orogenic period.

This retro-foreland was never an overfilled basin (sensu Covey, 1986) filled by large subsiding alluvial fans as expected by some stratigraphic models. As already mentioned, the megafans described here (‘Argiles à galets’ Fm) initiated during the Late Miocene (10.6 Ma) up to today, (1) resulted from a large uplift in response to a West European-scale

deformation and (2) recorded an overall sediment by-pass of the continental domain along steeper slopes generated by the uplift, feeding the deep-sea plain of the Bay of Biscay. The by-pass megafans do not represent the last 'overfilled' stage of the foreland evolution.

5.3. Building a sink preservation model in the foreland basin from active to post-foreland periods (Fig. 13)

Based on the Aquitaine retro-foreland example and its outlet to the Bay of Biscay deep-sea plain, we proposed a model for the evolution of the sink preservation in the foreland basins connected to a passive margin, from their subsiding period to post-orogenic uplifts. In this model, the foreland and upstream part of the margin (shelf and coastal plain) belong to same subsiding domain. The depositional profile, parallel to the mountain belt, is a platform on a continental crust passing to a continental slope and a deep-sea plain on oceanic crust.

The post-subsidence evolution of each foreland basin seems to be different (see the Introduction). This is mainly due to the inheritance (structure of the upper crust, existence of a decollement level(s), etc.) and the rate and amount of shortening. In the case of the Swiss Molassic Basin, the post-foreland evolution (Schlunnegger and Mosar, 2010; Willett and Schlunnegger, 2010) was characterized by the thrusting and uplift of the basin and the formation of a new orogenic wedge (the Jura Mountains) in front of the former foreland. In

the northern Alps, the end of the foreland did not coincide with the end of the shortening as in the case of the Aquitaine retro-foreland basin.

The key control factor is the balance between accommodation space created by the flexural subsidence [A_{sub}] and the siliciclastic sediment supply [S_{sc}]. Possible effects of the dynamic topography (e.g. Catuneanu, 2006) and therefore possible delays between the flexural and dynamic subsidence responses were not taken into account. Similarly, the effect of carbonate production was not considered here in the sediment budget. Three stages are defined.

- Stage 1: *foreland period* (both foredeep/forebulge and basin propagation of salt-controlled thrusts). When $\Delta A_{sub} \leq \Delta S_{sc}$ with low differences between ΔA_{sub} and ΔS_{sc}, the sediments are stored on the platform and no deposition occurred from the distal platform (condensation by downlap) to the deep-sea plain. Due to a slight imbalance in favour of ΔS_{sc}, the first order platform geometry is progradational-aggradational.
- Stage2: *post-foreland period 1 – subsiding platform*. When $\Delta A_{sub} < \Delta S_{sc}$ with significant differences between ΔA_{sub} and ΔS_{sc}, most of the sediments are transferred to the deep-sea plain with few preservations on the platform. The first order platform geometry is progradational with a low aggradational component.
- Stage 3: *post-foreland period 2 – by-pass and/or uplift of the platform*. When $\Delta A_{sub} << \Delta S_{sc}$ with $\Delta A_{sub} \leq 0$, all of the sediments are transferred to the deep-sea plain as deep-sea

fans. If $\Delta A_{sub} = 0$, the overall fluvial by-pass occurs on the platform and feeds pure progradational wedges. If $\Delta A_{sub} < 0$, uplift and overall fluvial erosion occurs on the platform and feeds forced progradational wedges.

In some foreland basins (e.g. Swiss Molassic Basin), stage 2 may be missing, with a direct transition from subsiding foreland (stage 1) to uplifted basin (stage 3). This model does not prejudge of the evolution of the shortening that may stop between stage 1 and 2 (case of the Aquitaine retro-foreland) or can still be happening during stage 3 (case of the Swiss Molassic Basin).

6. Conclusion

(1) *a new chronostratigraphic framework*: Four second order depositional sequences and at least 24 third order cycles have been identified, and an age model based on a combination of biostratigraphy, orbitostratigraphy and sequence stratigraphy with a time resolution of 0.1 Ma is proposed. From 50 Ma to today the duration of deposition, no deposition and erosion periods were quantified.

(2) *dating and wavelength assessment of the main phases of deformation of the retro-foreland from syn-orogenic to post-orogenic stages*:

- The end of the retroforeland activity and therefore the transition to a post-orogenic setting has been dated to the Chattian, ranging from 27.1 to 25.2 Ma.
- During the orogenic period, the transition from a foredeep/forebulge system to transported piggy-back basins occurred during Lutetian times. The shortening paroxysm of this medium wavelength deformation occurred during Priabonian times around 35.8 Ma.
- The post-orogenic period is marked by a major uplift of the Aquitaine Basin from Late Burdigalian (16.4 Ma) to Early Tortonian (10.6 Ma) in response to a possible mantle-controlled West European-scale uplift.

(3) *a reconstruction of the successive depositional profiles and related depositional topographies*: The type depositional profile up to the middle Miocene is a nearly flat coastal to alluvial plain characterized by an alternation of laterally extensive lakes and marshes with fine-grained fluvial channels. These nearly flat plains extended from the shorelines to the feet of the Pyrenees where they played the role of local base levels for alluvial fans. Since the Middle Miocene braided alluvial plains and low-preservation ('by-passing') megafans replaced these nearly flat plains.

977

978 (4) *a three step evolution of the Cenozoic sedimentation of the Aquitaine Basin - proposal of*

979 *a sink preservation model*:

980 • During the foreland period (foredeep then piggy-back) – here up to 25.2 Ma – when the

981 accommodation space created by the subsidence was balanced or slightly lower by/than

982 the siliciclastic sediment supply, most of the sediments are stored on the platform (here

983 the Aquitaine Basin). No sediments reached the deep-sea plain.

984 • During the post-foreland period (i.e. here at the end of the mountain belt shortening)

985 when the accommodation space created by the subsidence was lower than the

986 siliciclastic sediment supply and when the mountain belt reached its highest elevation

987 and erosion rate, most sediments are transferred and stored in the deep-sea plain of the

988 margin. Few sediments are preserved on the platform. In the case of the Pyrenees retro-

989 foreland, the Middle to Late Miocene West European-scale uplift enhanced this trend.

990

991

992 **Acknowledgements**

993

994 This work is part (and supported by) the 'Source-to-Sink compression' project that is jointly

995 managed by Total and the French geological survey BRGM. Biostratigraphic studies or

revaluations were performed by Speranta Popescu and Chantal Bourdillon from the GEOBIOSTRATDATA (SP) and ERADATA (CB) biostratigraphic service companies. We are very grateful to them. We also thank Sara Mullin for post-editing the English.

References

Sequence stratigraphy of siliciclastic systems - the ExxonMobil methodology: an atlas of exercices. In: Abreu, V., Neal, J., Bohacs, K., Kalbas, J. (Eds.), SEPM Concepts in Sedimentology and Paleontology, vol. 9. pp.226.

Allen, P.A., 2017. Sediment routing systems: The fate of sediment from source to sink. Cambridge University Press.

Allen, P.A., Allen, J.R., 2013. Basin analysis: Principles and application to petroleum play assessment. John Wiley & Sons Chichester.

Ambert, M., Ambert, P., 1995. Karstification des plateaux et encaissement des vallées au cours du Néogène et du Quaternaire dans les Grands Causses méridionaux (Larzac, Blandas). Géol. France, 37–50.

Anadón, P., Utrilla, R., Vázquez, A., 2000. Use of charophyte carbonates as proxy indicators of subtle hydrological and chemical changes in marl lakes: Example from the Miocene Bicorb Basin,

1015 eastern Spain. Sediment. Geol. 133, 325–347. https://doi.org/10.1016/S0037-0738(00)00047-6

1016 Angrand, P., Ford, M., Watts, A.B., 2018. Lateral Variations in Foreland Flexure of a Rifted Continental
1017 Margin: The Aquitaine Basin (SW France). Tectonics 37, 430–449.
1018 https://doi.org/10.1002/2017TC004670

1019 Antoine, P.-O., Duranthon, F., Tassy, P., 1997. L'apport des grands mammifères (Rhinocérotidés,
1020 Suoidés, Proboscidiens) à la connaissance des gisements du Miocène d'Aquitaine (France).
1021 Mem. Trav. E.P.H.E. Inst. Montpellier 21, pp. 581–590.

1022 Armitage, J.J., Allen, P.A., Burgess, P.M., Hampson, G.J., Whittaker, A.C., Duller, R.A., Michael, N.A.,
1023 2015. Sediment Transport Model For the Eocene Escanilla Sediment-Routing System:
1024 Implications For the Uniqueness of Sequence Stratigraphic Architectures. J. Sediment. Res. 85,
1025 1510–1524. https://doi.org/10.2110/jsr.2015.97

1026 Barruol, G., Granet, M., 2002. A Tertiary asthenospheric flow beneath the southern French Massif
1027 Central indicated by upper mantle seismic anisotropy and related to the west Mediterranean
1028 extension. Earth Planet. Sci. Lett. 202, 31–47.

1029 Beaumont, C., 1981. Foreland basins. Geophys. J. Int. 65, 291–329.

1030 Beaumont, C., J. A. Muñoz, J. Hamilton, and P. Fullsack 2000. Factors controlling the Alpine evolution
1031 of the central Pyrenees inferred from a
1032 comparison of observations and geodynamical models. J. Geophys. Res., 105(B4), 8121–8145,
1033 doi:10.1029/1999JB900390.

1034 Berger, J.P., Reichenbacher, B., Becker, D., Grimm, M., Grimm, K., Picot, L., Storni, A., Pirkenseer, C.,
1035 Derer, C., Schaefer, A., 2005. Paleogeography of the Upper Rhine Graben (URG) and the Swiss
1036 Molasse Basin (SMB) from Eocene to Pliocene. Int. J. Earth Sci. 94, 697–710.
1037 https://doi.org/10.1007/s00531-005-0475-2

1038 Bessin, P., Guillocheau, F., Robin, C., Braun, J., Bauer, H., Schroëtter, J.M., 2017. Quantification of
1039 vertical movement of low elevation topography combining a new compilation of global sea-
1040 level curves and scattered marine deposits (Armorican Massif, western France). Earth Planet.
1041 Sci. Lett. 470, 25–36. https://doi.org/10.1016/j.epsl.2017.04.018

1042 Biteau, J.-J., Le Marrec, A., Le Vot, M., Masset, J.-M., 2006. The Aquitaine Basin. Pet. Geosci. 12, 247–
1043 273. https://doi.org/10.1144/1354-079305-674

1044 Blair, T.C., McPherson, J.G., 2009. Processes and forms of alluvial fans, in: Geomorphology of Desert
1045 Environments. Springer Science+Business Media B.V., pp. 413–467.

1046 Bosch, G. V., Teixell, A., Jolivet, M., Labaume, P., Stockli, D., Domènech, M., Monié, P., 2016. Timing
1047 of Eocene-Miocene thrust activity in the Western Axial Zone and Chaînons Béarnais (west-
1048 central Pyrenees) revealed by multi-method thermochronology. Comptes Rendus Geosci. 348,
1049 246–256. https://doi.org/10.1016/j.crte.2016.01.001

1050 Bourrouilh, R., Richert, J., Zolnaï, G., 1995. The North Pyrenean Aquitaine Basin , France : Evolution
1051 and Hydrocarbons 1. AAPG Bull. 6, 831–853.

1052 Brault, N., Bourquin, S., Guillocheau, F., Dabard, M.P., Bonnet, S., Courville, P., Estéoule-Choux, J.,
1053 Stepanoff, F., 2004. Mio-Pliocene to Pleistocene paleotopographic evolution of Brittany

(France) from a sequence stratigraphic analysis: Relative influence of tectonics and climate. Sediment. Geol. 163, 175–210. https://doi.org/10.1016/S0037-0738(03)00193-3

Bremer, H., 1989. On the geomorphology of the South German scarplands. Catena 15, 45–67.

Brown Jr, L.F., Fisher, W.L., 1977. Seismic-Stratigraphic Interpretation of Depositional Systems: Examples from Brazilian Rift and Pull-Apart Basins: Section 2. Application of Seismic Reflection Configuration to Stratigraphic Interpretation. AAPG Mem. 26, pp. 213-248.

Cadenas, P., Fernández-Viejo, G., 2017. The Asturian Basin within the North Iberian margin (Bay of Biscay): seismic characterisation of its geometry and its Mesozoic and Cenozoic cover. Basin Res. 29, 521–541. https://doi.org/10.1111/bre.12187

Cahuzac, B., 1980. Stratigraphie et paléogéographie de l'Oligocène au Miocène moyen en Aquitaine sud-occidentale. Thèse, Université de Bordeaux 1.

Carminati, E., Cuffaro, M., Doglioni, C., 2009. Cenozoic uplift of Europe. Tectonics 28, TC4016.

Catuneanu, O., 2006. Principles of sequence stratigraphy. Elsevier.

Catuneanu, O., Abreu, V., Bhattacharya, J.P., Blum, M.D., Dalrymple, R.W., Eriksson, P.G., Fielding, C.R., Fisher, W.L., Galloway, W.E., Gibling, M.R., Giles, K.A., Holbrook, J.M., Jordan, R., Kendall, C.G.S.C., Macurda, B., Martinsen, O.J., Miall, A.D., Neal, J.E., Nummedal, D., Pomar, L., Posamentier, H.W., Pratt, B.R., Sarg, J.F., Shanley, K.W., Steel, R.J., Strasser, A., Tucker, M.E., Winker, C., 2009. Towards the standardization of sequence stratigraphy. Earth-Science Rev. 92, 1–33. https://doi.org/10.1016/j.earscirev.2008.10.003

1073 Catuneanu, O., Beaumont, C., Waschbusch, P., 1997. Interplay of static loads and subduction
1074 dynamics in foreland basins: Reciprocal stratigraphies and the “missing” peripheral bulge.
1075 Geology 25, 1087–1090.

1076 Cavelier, C., Fries, G., Lagarigue, J.L., Capdeville, J.P., 1997. Sedimentation progradante au
1077 Cenozoique inférieur en Aquitaine méridionale: un modèle. Géol. France, 69–79.

1078 Chevrot, S., Sylvander, M., Diaz, J., Martin, R., Mouthereau, F., Manatschal, G., Masini, E., Calassou,
1079 S., Grimaud, F., Pauchet, H., others, 2018. The non-cylindrical crustal architecture of the
1080 Pyrenees. Sci. Rep. 8, 9591.

1081 Clerc, C., Lagabrielle, Y., Labaume, P., Ringenbach, J.C., Vauchez, A., Nalpas, T., Bousquet, R., Ballard,
1082 J.F., Lahfid, A., Fourcade, S., 2016. Basement – Cover decoupling and progressive exhumation of
1083 metamorphic sediments at hot rifted margin. Insights from the Northeastern Pyrenean analog.
1084 Tectonophysics 686, 82–97. https://doi.org/10.1016/j.tecto.2016.07.022

1085 Cochelin, B., Lemirre, B., Denèle, Y., de Saint Blanquat, M., Lahfid, A., Duchêne, S., 2018. Structural
1086 inheritance in the Central Pyrenees: the Variscan to Alpine tectonometamorphic evolution of
1087 the Axial Zone. J. Geol. Soc. London. 175, 336–351. https://doi.org/10.1144/jgs2017-066

1088 Covey, M., 1986. The evolution of foreland basins to steady state: evidence from the western Taiwan
1089 foreland basin. International Association of Sedimentologists Spec. Pub. 8, pp. 77–90.

1090 Cremer, M., 1983. Approches sédimentologique et géophysique des accumulations turbiditiques:
1091 l’éventail profond du Cap-Ferret (Golfe de Gascogne), la série des grès d’Annot (Alpes-de-
1092 Haute-Provence). Thèse, Université de Bordeaux 1.

1093 Crouzel, C., 1957. Le Miocene du Bassin d'Aquitaine. Thèse, Université de Toulouse.

1094 Curry, M.E., van der Beek, P., Huismans, R.S., Wolf, S.G., Muñoz, J.-A., 2019. Evolving
1095 paleotopography and lithospheric flexure of the Pyrenean Orogen from 3D flexural modeling
1096 and basin analysis. Earth Planet. Sci. Lett. 515, 26–37.

1097 DeCelles, P.G., Giles, K.A., 1996. Foreland basin systems. Basin Res. 8, 105–123.

1098 Define, E., Pastre, J.-F., Lageat, Y., Cantagrel, J.-M., Meloux, J.-L., 2007. L'évolution géomorphologique
1099 néogène de la haute vallée de la Loire comparée à celle de l'Allier. In : Du continent au basin
1100 versant. Théorie et pratique en géographie physique. Presses Universitaires Blaise-Pascal,
1101 Clermont-Ferrand, pp. 469-484.

1102 Desegaulx, P., Kooi, H., Cloetingh, S., 1991. Consequences of foreland basin development on thinned
1103 continental lithosphere: application to the Aquitaine basin (SW France). Earth Planet. Sci. Lett.
1104 106, 116–132.

1105 Desegaulx, Pa., Brunet, M.-Fran., 1990. Tectonic subsidence of the Aquitaine basin since Cretaceous
1106 times. Bull. Soc. Géol. France 8, 295–306.

1107 Dickinson, W.R., 1974. Plate tectonics and sedimentation. SEPM Spec. Pub. 22, pp. 1-27

1108 Dubarry, R., 1988. Interpretation dynamique du paléocène et de l'éocène inférieur et moyen de la
1109 région de pau-Tarbes (avant-pays nord des Pyrénées occidentales, sw France): Sédimentologie,
1110 corrélations dia graphiques, décompaction et calculs de subsidence. Thèse de 3ème Cycle, Pau.

1111 Dubreuilh, J., Capdeville, J.P., Farjanel, G., Karnay, G., Platel, J.P., Simon-Coinçon, R., 1995.

1112 Dynamique d'un comblement continental néogène et quaternaire: l'exemple du bassin
1113 d'Aquitaine. Géol. France, 3–26.

1114 Espurt, N., Angrand, P., Teixell, A., Labaume, P., Ford, M., de Saint Blanquat, M., Chevrot, S., 2019.
1115 Crustal-scale balanced cross-section and restorations of the Central Pyrenean belt (Nestes-Cinca
1116 transect): Highlighting the structural control of Variscan belt and Permian-Mesozoic rift systems
1117 on mountain building. Tectonophysics 764, 25–45. https://doi.org/10.1016/j.tecto.2019.04.026

1118 Fernández-Viejo, G., Pulgar, J.A., Gallastegui, J., Quintana, L., 2012. The Fossil Accretionary Wedge of
1119 the Bay of Biscay: Critical Wedge Analysis on Depth-Migrated Seismic Sections and
1120 Geodynamical Implications. J. Geol. 120, 315–331. https://doi.org/10.1086/664789

1121 Ferrer, O., Jackson, M.P.A., Roca, E., Rubinat, M., 2012. Evolution of salt structures during extension
1122 and inversion of the Offshore Parentis Basin (Eastern Bay of Biscay). Geol. Soc. London, Spec.
1123 Publ. 363, 361–380.

1124 Fillon, C., van der Beek, P., 2012. Post-orogenic evolution of the southern Pyrenees: Constraints from
1125 inverse thermo-kinematic modelling of low-temperature thermochronology data. Basin Res. 24,
1126 418–436. https://doi.org/10.1111/j.1365-2117.2011.00533.x

1127 Fitzgerald, PG., Muñoz, J.A., Coney, P.J., Baldwin, S.L. 1999. Asymmetric exhumation across the
1128 Pyrenean Orogen; implications for the tectonic evolution of a collisional orogen. Earth planet
1129 Sci. Lett. 173, 157-170.

1130 Flemings, P.B., Jordan, T.E., 1989. A synthetic stratigraphic model of foreland basin development. J.
1131 Geophys. Res. Solid Earth 94, 3851–3866.

1132 Ford, M., Hemmer, L., Vacherat, A., Gallagher, K., Christophoul, F., 2016. Retro-wedge foreland basin
1133 evolution along the ECORS line, eastern Pyrenees, France. J. Geol. Soc. Lond. 173, 419-437.

1134 Gallastegui, J., Pulgar, J.A., Gallart, J., 2002. Initiation of an active margin at the North Iberian
1135 continent-ocean transition. Tectonics 21, 11–15.

1136 Gardère, P., 2005. La Formation des Sables Fauves: dynamique sédimentaire au Miocène moyen et
1137 évolution morpho-structurale de l'Aquitaine (SW France) durant le Néogène. Eclogae Geol.
1138 Helv. 98, 201–217.

1139 Gardère, P., Rey, J., Duranthon, F., 2002. Les "Sables fauves", témoins de mouvements tectoniques
1140 dans le bassin d'Aquitaine au Miocène moyen. Comptes Rendus Géoscience 334, 987–994.

1141 Gibson, M., H. D. Sinclair, G. J. Lynn, and F. M. Stuart (2007), Late- to post-orogenic exhumation of
1142 the central Pyrenees revealed through
1143 combined thermochronological data and modelling, Basin Res., 19, 323–334, doi:10.1111/j.1365-
1144 2117.2007.00333.x.

1145 Gierlowski-Kordesch, E.H., 2010. Lacustrine Carbonates, Developments in Sedimentology 61, Elsevier,
1146 pp. 1-101. https://doi.org/10.1016/S0070-4571(09)06101-9

1147 Gómez, M., Vergés, J., Riaza, C., 2002. Inversion tectonics of the northern margin of the Basque
1148 Cantabrian Basin. Bull. la Société géologique Fr. 173, 449–459.

1149 Gourdon-Platel, N., PLATEL, J.P., Astruc, J.G., 2000. La formation de Rouffignac, témoin d'une
1150 paléoaltérite cuirassée intra-éocène en Périgord-Quercy. Géol. France. 1, 65–76.

1151 Graciansky, P.C. de, Hardenbol, J., Jacquin, T., Vail, P.R., 1998. Mesozoic and Cenozoic Sequence
1152 Stratigraphy of Eurpoean Basins, SEPM Special Pub. 60, pp. 786.

1153 Gradstein, F.M., Ogg, J.G., Schmitz, M., Ogg, G., 2012. The geologic time scale 2012. Elsevier.

1154 Granet, M, Stoll, G., Dorel, J., Achauer, U., Poupinet, G., Fuchs, K., 1995. Massif Central (France): new
1155 constraints on the geodynamical evolution from teleseismic tomography. Geophys. J. Int. 121,
1156 33–48.

1157 Granet, Michel, Wilson, M., Achauer, U., 1995. Imaging a mantle plume beneath the French Massif
1158 Central. Earth Planet. Sci. Lett. 136, 281–296.

1159 Guillocheau, F., Brault, N., Thomas, E., Barbarand, J., others, 2003. Histoire géologique du massif
1160 Armoricain depuis 140 Ma (Crétacé-Actuel). Bull. Inf. Géol. Bass. Paris 40, 13-28.

1161 Gurnis, M., 1992. Rapid continental subsidence following the initiation and evolution of subduction.
1162 Science 255, 1556–1558.

1163 Handford, C.R., Loucks, R.G., 1993. Carbonate Depositional Sequences and Systems Tracts-Responses
1164 of Carbonate Platforms to Relative Sea-Level Changes. AAPG Mem. 57, pp. 3-41

1165 Haq, B.U., Hardenbol, J.A.N., Vail, P.R., 1987. Chronology of fluctuating sea levels since the Triassic.
1166 Science 235, 1156–1167.

1167 Haq, B.U., Hardenbol, J., Vail, P.R., 1988. Mesozoic and Cenozoic chronostratigraphy and cycles of
1168 sea-level change. SEPM Spec. Pub. 42, pp. 71-108.

1169 Hardenbol, J.A.N., Thierry, J., Farley, M.B., Jacquin, T., De Graciansky, P.-C., Vail, P.R., 1998. Mesozoic

and Cenozoic sequence chronostratigraphic framework of European basins. SEPM Special Pub. 60, pp. 3-13.

Helland-Hansen, W., Gjelberg, J.G., 1994. Conceptual basis and variability in sequence stratigraphy: a different perspective. Sediment. Geol. 92, 31–52. https://doi.org/10.1016/0037-0738(94)90053-1

Helland-Hansen, W., Hampson, G.J., 2009. Trajectory analysis: Concepts and applications. Basin Res. 21, 454–483. https://doi.org/10.1111/j.1365-2117.2009.00425.x

Helland-Hansen, W., Martinsen, O.J., 1996. Shoreline trajectories and sequences; description of variable depositional-dip scenarios. J. Sediment. Res. 66, 670–688.

Homewood, P., Allen, P.A., Williams, G.D., 1986. Dynamics of the Molasse Basin of western Switzerland, in: Foreland Basins. International Association of Sedimentologists Spec. Pub. 8, pp. 199–217.

Hunt, D., Tucker, M.E., 1992. Stranded parasequences and the forced regressive wedge systems tract: deposition during base-level fall. Sediment. Geol. 81, 1–9.

Huyghe, D., F. Mouthereau, and L. Emmanuel, 2012a, Oxygen isotopes of marine mollusc shells record Eocene elevation change in the Pyrenees. Earth planet Sci. Lett., 345-348(C)

Jervey, M.T., 1988. Quantitative geological modeling of siliciclastic rock sequences and their seismic expression. SEPM Spec. Pub. 42, 47–69. https://doi.org/10.2110/pec.88.01.0047

Johnson, D.D., Beaumont, C., 1995. Preliminary results from a planform kinematic model of orogen

1189 evolution, surface processes and the development of clastic foreland basin stratigraphy. SEPM
1190 Spec. Pub. 52, pp. 3-24.

1191 Jones, D.K.C., 1980. The Tertiary evolution of south-east England with particular reference to the
1192 Weald, in: The Shaping of Southern England. Academic Press London, pp. 13–47.

1193 Kruit, C., Brouwer, J., Ealey, P., 1972. A deep-water sand fan in the Eocene Bay of Biscay. Nature
1194 Phys. Sci. 240, 59–61.

1195 Lagabrielle, Y., Labaume, P., de Saint Blanquat, M., 2010. Mantle exhumation, crustal denudation,
1196 and gravity tectonics during Cretaceous rifting in the Pyrenean realm (SW Europe): Insights
1197 from the geological setting of the lherzolite bodies. Tectonics 29., TC4012.

1198 Le Pochat, G., 1984. Bassins paléozoiques cachés sous l'Aquitaine. Doc. du Bur. Rech. Géol. Min. 80,
1199 79–86.

1200 Masini, E., Manatschal, G., Tugend, J., Mohn, G., Flament, J.-M., 2014. The tectono-sedimentary
1201 evolution of a hyper-extended rift basin: the example of the Arzacq--Mauléon rift system
1202 (Western Pyrenees, SW France). Int. J. Earth Sci. 103, 1569–1596.

1203 Mathieu, C., 1986. Histoire géologique du sous-bassin de Parentis. Bull. Centres Rech. Explor. Elf-
1204 Aquitaine 10, 22–47.

1205 Miall, A.D., 1981. Alluvial sedimentary basins: tectonic setting and basin architecture. In: Miall, A.D.
1206 Sedimentation and tectonics in alluvial basins. Geological Association of Canada Special Paper.
1207 23, 1-33.

1208 Michael, Nikolaos A., Carter, A., Whittaker, A.C., Allen, P.A., 2014. Erosion rates in the source region
1209 of an ancient sediment routing system: comparison of depositional volumes with
1210 thermochronometric estimates. J. Geol. Soc. London. 171, 401–412.
1211 https://doi.org/10.1144/jgs2013-108

1212 Michael, N.A., Whittaker, A.C., Allen, P.A., 2013. The Functioning of Sediment Routing Systems Using
1213 a Mass Balance Approach: Example from the Eocene of the Southern Pyrenees. J. Geol. 121,
1214 581–606. https://doi.org/10.1086/673176

1215 Michael, Nikolas A., Whittaker, A.C., Carter, A., Allen, P.A., 2014. Volumetric budget and grain-size
1216 fractionation of a geological sediment routing system: Eocene Escanilla Formation, south-
1217 central Pyrenees. Bull. Geol. Soc. Am. 126, 585–599. https://doi.org/10.1130/B30954.1

1218 Miller, K., Wright, J., Katz, M., Browning, J., Cramer, B., Wade, B., Mizintseva, S., 2008. A View of
1219 Antarctic Ice-Sheet Evolution from Sea-Level and Deep-Sea Isotope Changes During the Late
1220 Cretaceous-Cenozoic. In: Antarctica: A Keystone in a Changing World, Nat. Acad. Press
1221 Washington DC, pp. 55–70.

1222 Miller, K.G., Miller, K.G., Kominz, M.A., Browning, J. V, Wright, J.D., Mountain, G.S., Katz, M.E.,
1223 Sugarman, P.J., Cramer, B.S., Christie-blick, N., Pekar, S.F., 2005. The Phanerozoic Record of
1224 Global Sea-Level Change. Science. 310, 1293–1298. https://doi.org/10.1126/science.1116412

1225 Miller, K.G., Mountain, G.S., Wright, J.D., Browning, J. V, 2011. A 180 Million Year Record of Sea Level
1226 and Ice Volume Variations. Oceanography 24, 40–53.
1227 https://doi.org/10.5670/oceanog.2011.26.COPYRIGHT

1228 Mitchum Jr, R.M., Vail, P.R., Sangree, J.B., 1977. Seismic stratigraphy and global changes of sea level:
1229 Part 6. Stratigraphic interpretation of seismic reflection patterns in depositional sequences:
1230 Section 2. Application of seismic reflection configuration to stratigraphic interpretation. AAPG
1231 Mem. 26, pp. 53-62.

1232 Mitrovica, J.X., Beaumont, C., Jarvis, G.T., 1989. Tilting of continental interiors by the dynamical
1233 effects of subduction. Tectonics 8, 1079–1094.

1234 Mouthereau, F., Vacherat, A., Lacombe, O., Christophoul, F., Filleaudeau, P.-Y., Pik, R., Fellin, M.G.,
1235 Castelltort, S., Masini, E., 2014. Placing limits to shortening evolution in the Pyrenees: Role of
1236 margin architecture and implications for the Iberia/Europe convergence. Tectonics 33, 2283–
1237 2314. https://doi.org/10.1002/2014TC003663

1238 Mudie, P.J., Marret, F., Mertens, K.N., Shumilovskikh, L., Leroy, S.A.G., 2017. Atlas of modern
1239 dinoflagellate cyst distributions in the Black Sea Corridor: from Aegean to Aral Seas, including
1240 Marmara, Black, Azov and Caspian Seas. Mar. Micropaleontol. 134, 1–152.
1241 https://doi.org/10.1016/j.marmicro.2017.05.004

1242 Naylor, M., Sinclair, H.D., 2008. Pro- vs. retro-foreland basins. Basin Res. 20, 285–303.
1243 https://doi.org/10.1111/j.1365-2117.2008.00366.x

1244 Neal, J., Abreu, V., 2009. Sequence stratigraphy hierarchy and the accommodation succession
1245 method. Geology 37, 779–782. https://doi.org/10.1130/G25722A.1

1246 Nehlig, P., Leyrit, H., Dardon, A., Freour, G., de Goer de Herve, A., Huguet, D., Thieblemont, D., 2005.
1247 Constructions et destructions du stratovolcan du Cantal. Bull. Soc. Geol. France 172, 295–308.

https://doi.org/10.2113/172.3.295

Paris, F., Le Pochat, G., 1994. The Aquitaine Basin, in: Pre-Mesozoic Geology in France and Related Areas. Springer, pp. 405–415.

Patruno, S., Helland-Hansen, W., 2018. Clinoform systems: Review and dynamic classification scheme for shorelines, subaqueous deltas, shelf edges and continental margins. Earth-Science Rev. 185, 202–233. https://doi.org/10.1016/j.earscirev.2018.05.016

Plint, A.G., Nummedal, D., 2000. The falling stage systems tract: recognition and importance in sequence stratigraphic analysis. Geol. Soc. London, Spec. Publ. 172, 1–17. https://doi.org/10.1144/GSL.SP.2000.172.01.01

Ponte, J.P., Robin, C., Guillocheau, F., Popescu, S., Suc, J.P., Dall'Asta, M., Melinte-Dobrinescu, M.C., Bubik, M., Dupont, G., Gaillot, J., 2019. The Zambezi delta (Mozambique channel, East Africa): High resolution dating combining bio- orbital and seismic stratigraphies to determine climate (palaeoprecipitation) and tectonic controls on a passive margin. Mar. Pet. Geol. 105, 293–312. https://doi.org/10.1016/j.marpetgeo.2018.07.017

Posamentier, H.W., Allen, G.P., 1993. Siliciclastic sequence stratigraphic patterns in foreland, ramp-type basins. Geology 21, 455–458.

Posamentier, H.W., Jervey, M.T., Vail, P.R., 1988. Eustatic controls on clastic deposition I—conceptual framework. In: Wilgus, C.K., Hastings, B.S., Kendall, C.G.StC., Posamentier, H.W., Ross, C.A., Van Wagoner, J.C. (Eds.), Sea Level Changes: an Intregrated Approach, SEPM Spec. Pub. 42, pp. 109-124.

1268 Posamentier, H.W., Vail, P.R., 1988. Eustatic Controls on Clastic Deposition II—Sequence and Systems
1269 Tract Models. In: Wilgus, C.K., Hastings, B.S., Kendall, C.G.StC., Posamentier, H.W., Ross, C.A.,
1270 Van Wagoner, J.C. (Eds.), Sea Level Changes: an Intregrated Approach, SEPM Spec. Pub. 42, pp.
1271 125–154.

1272 Puigdefàbregas, C., Souquet, P., 1986. Tecto-sedimentary cycles and depositional sequences of the
1273 Mesozoic and Tertiary from the Pyrenees. Tectonophysics 129, 173–203.

1274 Robin, C., Guillocheau, F., Gaulier, J.-M., 1998. Discriminating between tectonic and eustatic controls
1275 on the stratigraphic record in the Paris basin. Terra Nov. 10, 323–329.

1276 Roca, E., Muñoz, J.A., Ferrer, O., Ellouz, N., 2011. The role of the Bay of Biscay Mesozoic extensional
1277 structure in the configuration of the Pyrenean orogen: Constraints from the MARCONI deep
1278 seismic reflection survey. Tectonics 30, 1–33. https://doi.org/10.1029/2010TC002735

1279 Rocher, M., Lacombe, O., Angelier, J., Deffontaines, B., Verdier, F., 2000. Cenozoic folding and
1280 faulting in the south Aquitaine Basin (France): Insights from combined structural and
1281 paleostress analyses. J. Struct. Geol. 22, 627–645. https://doi.org/10.1016/S0191-
1282 8141(99)00181-9

1283 Roest, W.R., Srivastava, S.P., 1991. Kinematics of the plate boundaries between Eurasia, Iberia, and
1284 Africa in the North Atlantic from the Late Cretaceous to the present. Geology 19, 613–616.

1285 Roure, F., Choukroune, P., Berastegui, X., Munoz, J.A., Villien, A., Matheron, P., Bareyt, M., Seguret,
1286 M., Camara, P., Deramond, J., 1989. ECORS deep seismic data and balanced cross sections:
1287 Geometric constraints on the evolution of the Pyrenees. Tectonics 8, 41–50.

1288 Saspiturry, N., Razin, P., Baudin, T., Serrano, O., Issautier, B., Lasseur, E., Allanic, C., Thinon, I., Leleu,
1289 S., 2019. Symmetry vs. asymmetry of a hyper-thinned rift: Example of the Mauléon Basin
1290 (Western Pyrenees, France). Mar. Pet. Geol. 104, 86–105.
1291 https://doi.org/10.1016/j.marpetgeo.2019.03.031

1292 Schettino, A., Turco, E., 2011. Tectonic history of the Western Tethys since the Late Triassic. Bull.
1293 Geol. Soc. Am. 123, 89–105. https://doi.org/10.1130/B30064.1

1294 Schlunegger, F., Mosar, J., 2011. The last erosional stage of the Molasse Basin and the Alps. Int. J.
1295 Earth Sci. 100, 1147–1162. https://doi.org/10.1007/s00531-010-0607-1

1296 Schoeffler, J., 1971. Etude structurale des terrains molassiques du piedmont-nord des Pyrénées de
1297 Peyrehorade à Carcassonne. Thèse, Université de Bordeaux 1.

1298 Serrano, O., 2001. Le Crétacé Supérieur-Paléogène du Bassin Compressif Nord-Pyrénéen (Bassin de
1299 l'Adour). Sédimentologie, Stratigraphie, Géodynamique. Thèse de 3ème Cycle, Université Rennes
1300 1. and Mem. Géosciences Rennes 101.

1301 Serrano, O., Guillocheau, F., Leroy, E., 2001. Évolution du bassin compressif Nord-Pyrénéen au
1302 paléogène (basin de l'Adour): Contraintes stratigraphiques. Comptes Rendus l'Academie Sci. -
1303 Ser. IIa Sci. la Terre des Planetes 332, 37–44. https://doi.org/10.1016/S1251-8050(00)01487-7

1304 Shukla, U.K., Singh, I.B., Sharma, M., Sharma, S., 2001. A model of alluvial megafan sedimentation:
1305 Ganga Megafan. Sediment. Geol. 144, 243–262.

1306 Sinclair, H.D., Allen, P.A., 1992. Vertical versus horizontal motions in the Alpine orogenic wedge:

1307 stratigraphic response in the foreland basin. Basin Res. 4, 215–232.

1308 Sinclair, H.D., Coakley, B.J., Allen, P.A., Watts, A.B., 1991. Simulation of foreland basin stratigraphy
1309 using a diffusion model of mountain belt uplift and erosion: an example from the central Alps,
1310 Switzerland. Tectonics 10, 599–620.

1311 Sinclair, H. D., M. Gibson, M. Naylor, and R. G. Morris 2005. Asymmetric growth of the Pyrenees
1312 revealed through measurement and
1313 modeling of orogenic fluxes. Am. J. Sci., 305(May), 369–406.

1314 Singh, H., Parkash, B., Gohain, K., 1993. Facies analysis of the Kosi megafan deposits. Sediment. Geol.
1315 85, 87–113.

1316 Stanistreet, I.G., McCarthy, T.S., 1993. The Okavango Fan and the classification of subaerial fan
1317 systems. Sediment. Geol. 85, 115–133.

1318 Sztrákos, K., Steurbaut, E., 2017. Révision lithostratigraphique et biostratigraphique de l'oligocène
1319 d'aquitaine occidentale (France). Geodiversitas 39, 741–781.
1320 https://doi.org/10.5252/g2017n4a6

1321 Sztrákos, K., Blondeau, A., Hottinger, L., 2010. Lithostratigraphie et biostratigraphie des formations
1322 marines paléocènes et éocènes nord-aquitaines (bassin de Contis et Parentis, seuil et plate-
1323 forme nord-aquitaines), Foraminifères éocènes du bassin d'Aquitaine. Géol. France, 3-52.

1324 Sztrákos, K., Gély, J.P., Blondeau, A., Müller, C., 1998. L'Éocène du Bassin sud-aquitain:
1325 lithostratigraphie, biostratigraphie et analyse séquentielle. Géol. France, 57–105.

1326 Sztrákos, K., Gély, J.P., Blondeau, A., Müller, C., 1997. Le Paléocène et l'Ilerdien du Bassin sud-
1327 aquitain: lithostratigraphie et analyse séquentielle. Géol. France, 27-54.

1328 Teixell, A., Labaume, P., Ayarza, P., Espurt, N., de Saint Blanquat, M., Lagabrielle, Y., 2018. Crustal
1329 structure and evolution of the Pyrenean-Cantabrian belt: A review and new interpretations
1330 from recent concepts and data. Tectonophysics 724–725, 146–170.
1331 https://doi.org/10.1016/j.tecto.2018.01.009

1332 Teixell, A., Labaume, P., Lagabrielle, Y., 2016. The crustal evolution of the west-central Pyrenees
1333 revisited: inferences from a new kinematic scenario. Comptes Rendus Geosci. 348, 257–267.

1334 Thinon, I., 1999. Structure profonde de la marge nord-Gascogne et du bassin armoricain. Thèse de
1335 3ème Cycle, Université de Brest.

1336 Thinon, I., Fidalgo-González, L., Réhault, J.-P., Olivet, J.-L., 2001. Déformations pyrénéennes dans le
1337 golfe de Gascogne. Comptes Rendus Acad. Sci. Paris, Sér.IIA-Earth Planet. Sci. 332, 561–568.

1338 Thinon, I., Réhault, J.-P., Fidalgo-Gonzales, L., 2002. La couverture sédimentaire syn-rift de la marge
1339 nord Gascogne et du Bassin armoricain (golfe de Gascogne) à partir de nouvelles données de
1340 sismique-réflexion. Bull. Soc. Géol. France 173, 515-522.

1341 Tugend, J., Manatschal, G., Kusznir, N.J., Masini, E., 2015. Characterizing and identifying structural
1342 domains at rifted continental margins: application to the Bay of Biscay margins and its Western
1343 Pyrenean fossil remnants. Geol. Soc. London, Spec. Publ. 413, 171–203.

1344 Tugend, J., Manatschal, G., Kusznir, N.J., Masini, E., Mohn, G., Thinon, I., 2014. Formation and

1345 deformation of hyperextended rift systems: Insights from rift domain mapping in the Bay of
1346 Biscay-Pyrenees. Tectonics 33, 1239–1276.

1347 Vacherat, A., Mouthereau, F., Pik, R., Huyghe, D., Paquette, J.L., Christophoul, F., Loget, N., Tibari, B.,
1348 2017. Rift-to-collision sediment routing in the Pyrenees: A synthesis from sedimentological,
1349 geochronological and kinematic constraints. Earth-Science Rev. 172, 43–74.
1350 https://doi.org/10.1016/j.earscirev.2017.07.004

1351 Vail, P.R., Audermard, S.A., Bowman, P.N., Eisner, G., 1991. The stratigraphy signatures of tectonics,
1352 eustasy and sedimentology. In: Cycles and Events in Stratigraphy, Springer-Verlag Berlin,pp. 617
1353 – 659.

1354 Vail, P.R., Mitchum Jr, R.M., Thompson III, S., 1977. Seismic stratigraphy and global changes of sea
1355 level: Part 3. Relative changes of sea level from Coastal Onlap: section 2. Application of seismic
1356 reflection Configuration to Stratigrapic Interpretation. AAPG Mem. 26, pp. 63-82.

1357 Van Wagoner, J.C., Mitchum, R.M., Campion, K.M., Rahmanian, V.D., 1990. Siliciclastic sequence
1358 stratigraphy in well logs, cores, and outcrops: concepts for high-resolution correlation of time
1359 and facies. AAPG Methods in Exploration Series 7.

1360 Vergés, J., Fernández, M., Martìnez, A., 2002. The Pyrenean orogen: Pre-, syn-, and post-collisional
1361 evolution. J. Virtual Explor. 8, 55–74. https://doi.org/10.3809/jvirtex.2002.00058

1362 Vergés, J., Garcia-Senz, J., 2001. Mesozoic evolution and Cenozoic inversion of the Pyrenean rift.
1363 Mém. Muséum Nat. Hist. Nat. Paris 186, 187–212.

1364 Warren, J.K., 2010. Evaporites through time: Tectonic, climatic and eustatic controls in marine and
1365 nonmarine deposits. Earth-Science Rev. 98, 217–268.
1366 https://doi.org/10.1016/j.earscirev.2009.11.004

1367 Willett, S.D., Schlunegger, F., 2010. The last phase of deposition in the Swiss Molasse Basin: From
1368 foredeep to negative-alpha basin. Basin Res. 22, 623–639. https://doi.org/10.1111/j.1365-
1369 2117.2009.00435.x

1370 Winnock, E., 1973. Expose succinct de l'evolution paleogeologique de l'Aquitaine. Bull. Soc. Géol.
1371 France 7, 5–12.

1372 Zachos, J., Pagani, M., Sloan, L., Thomas, E., Billups, K., 2001. Trends, rhythms, and aberrations in
1373 global climate 65 Ma to present. Science. 292, 686–693.

1374 Ziegler, P.A., 1990. Geological atlas of western and central Europe. SHELL Internationale Petroleum
1375 Maatschappij B.V. The Hague.

1376 Ziegler, P.A., Dèzes, P., 2007. Cenozoic uplift of Variscan Massifs in the Alpine foreland: Timing and
1377 controlling mechanisms. Glob. Planet. Change 58, 237–269.

1378

1379 **Figure and table captions**

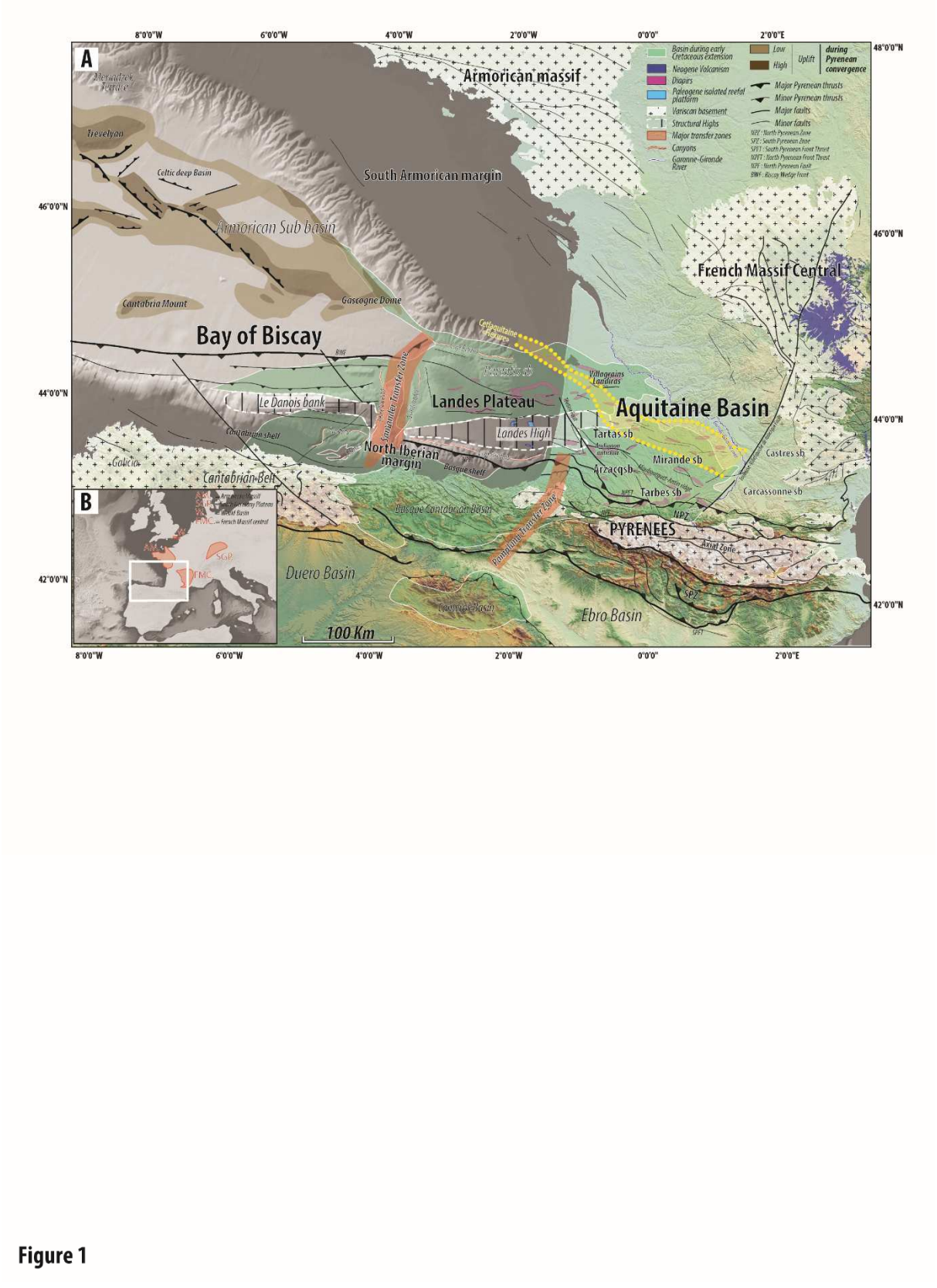

Figure 1

1380

1381 **Fig. 1**. A: Location of the studied area in Europe. B: Main physiographic and structural

1382 features of the Aquitaine Basin, Landes Plateau and Bay of Biscay deep-basin.

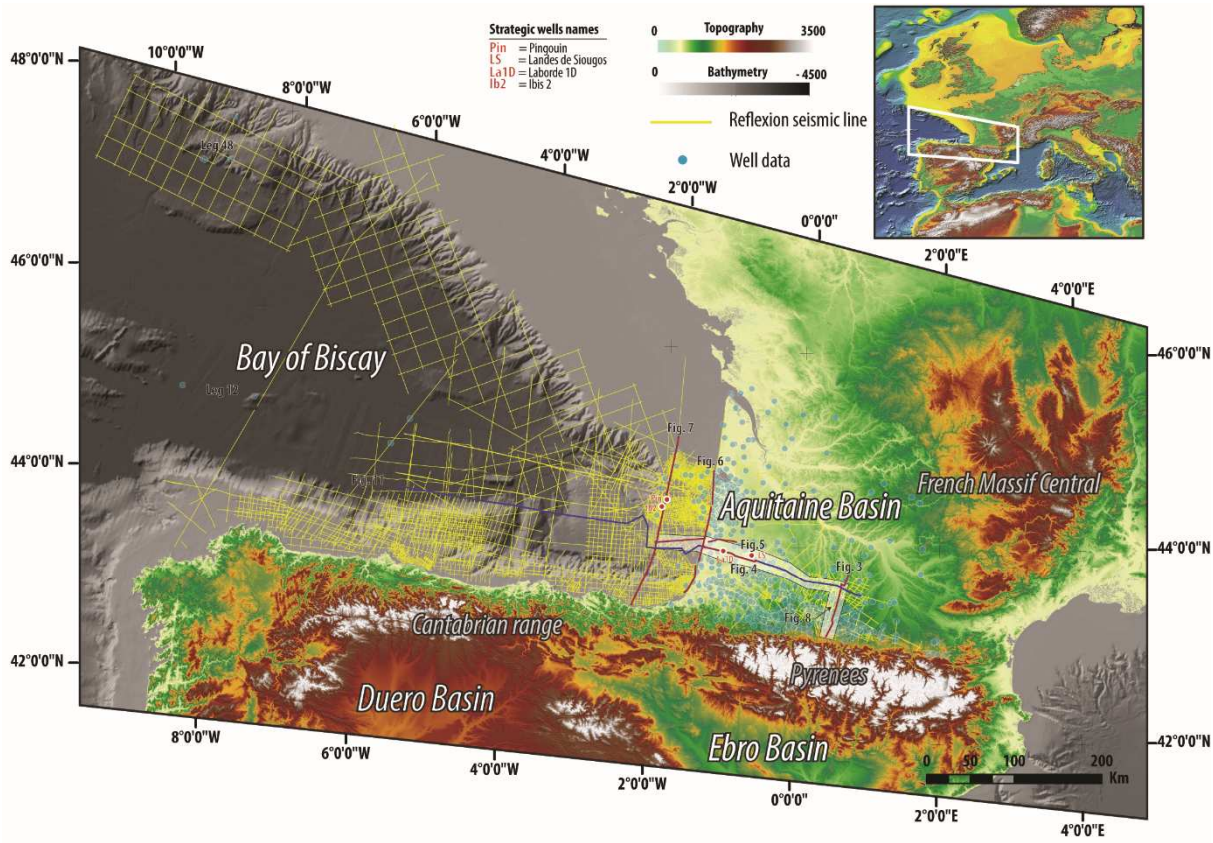

1383 **Figure 2**

1384 **Fig. 2**. Dataset for the seismic reflection lines and location of the dated wells and seismic

1385 lines shown in this study.

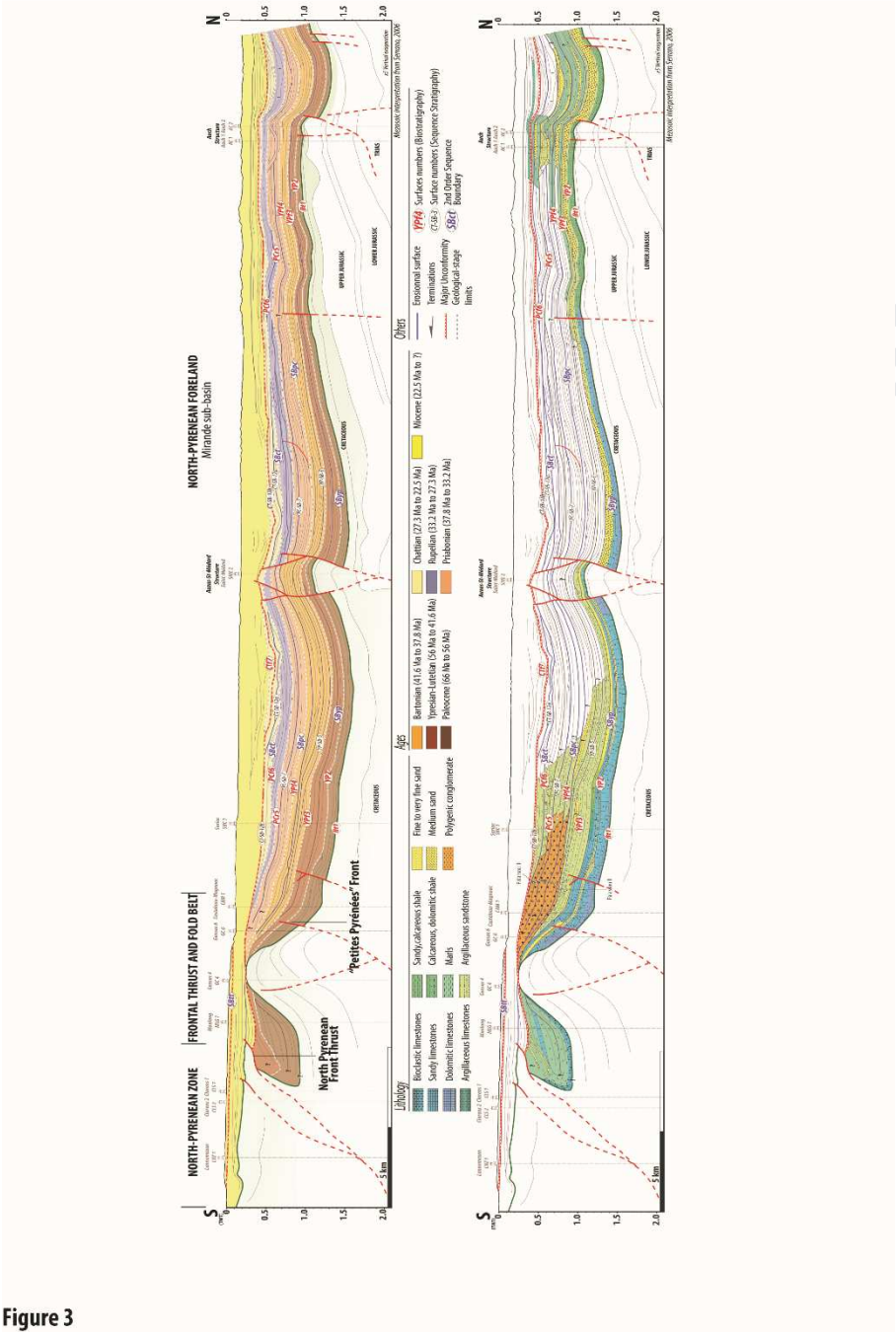

1386 **Figure 3**

1387 **Fig. 3**. Sequence stratigraphic and structural interpretation of the onshore seismic line LR6

1388 (see Fig. 2 for location) crossing the North Pyrenean and 'Petites Pyrénées' Fronts –

1389 Mesozoic geometries from Serrano et al. (2006).

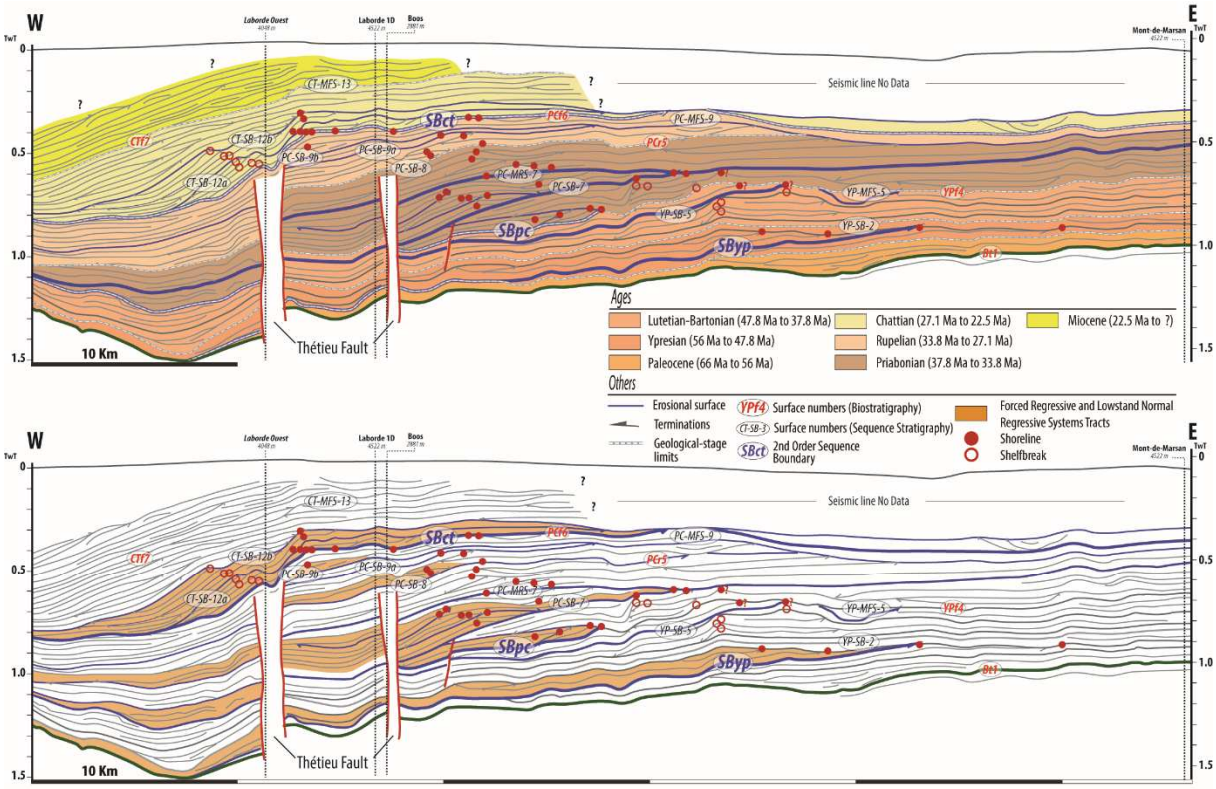

1390 **Figure 4**

1391 **Fig. 4**. Sequence stratigraphic and structural interpretation of the onshore seismic line LR11

1392 (see Fig. 2 for location)

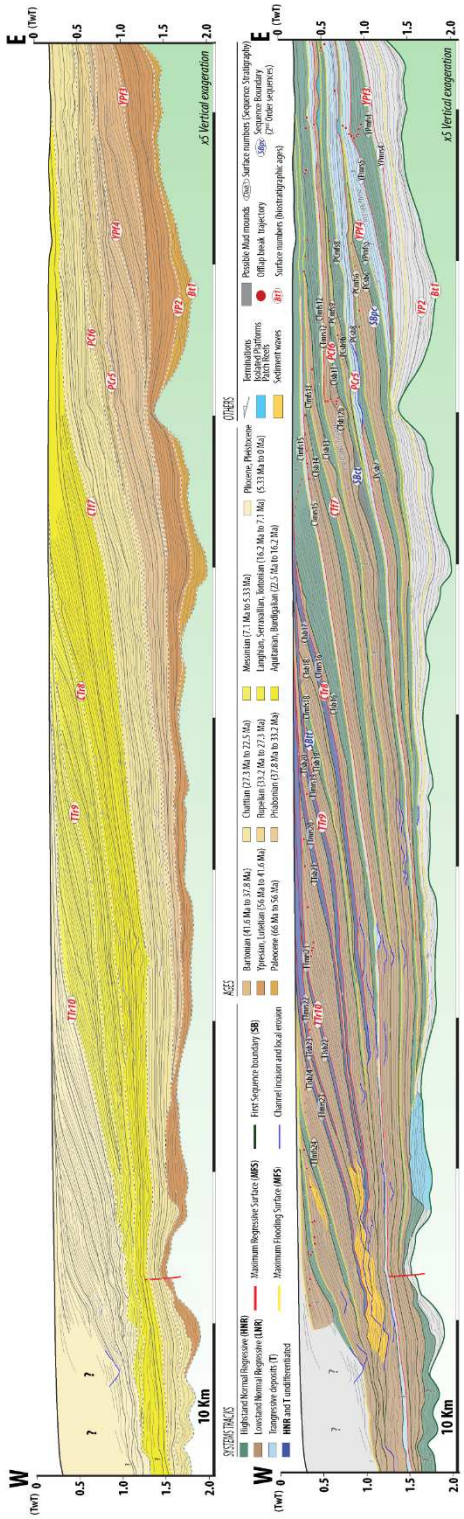

1393 **Figure 5**

1394 **Fig. 5**. Sequence stratigraphic and structural interpretation of the 'offshore Mimizan Lake'

1395 seismic line (see Fig. 2 for location).

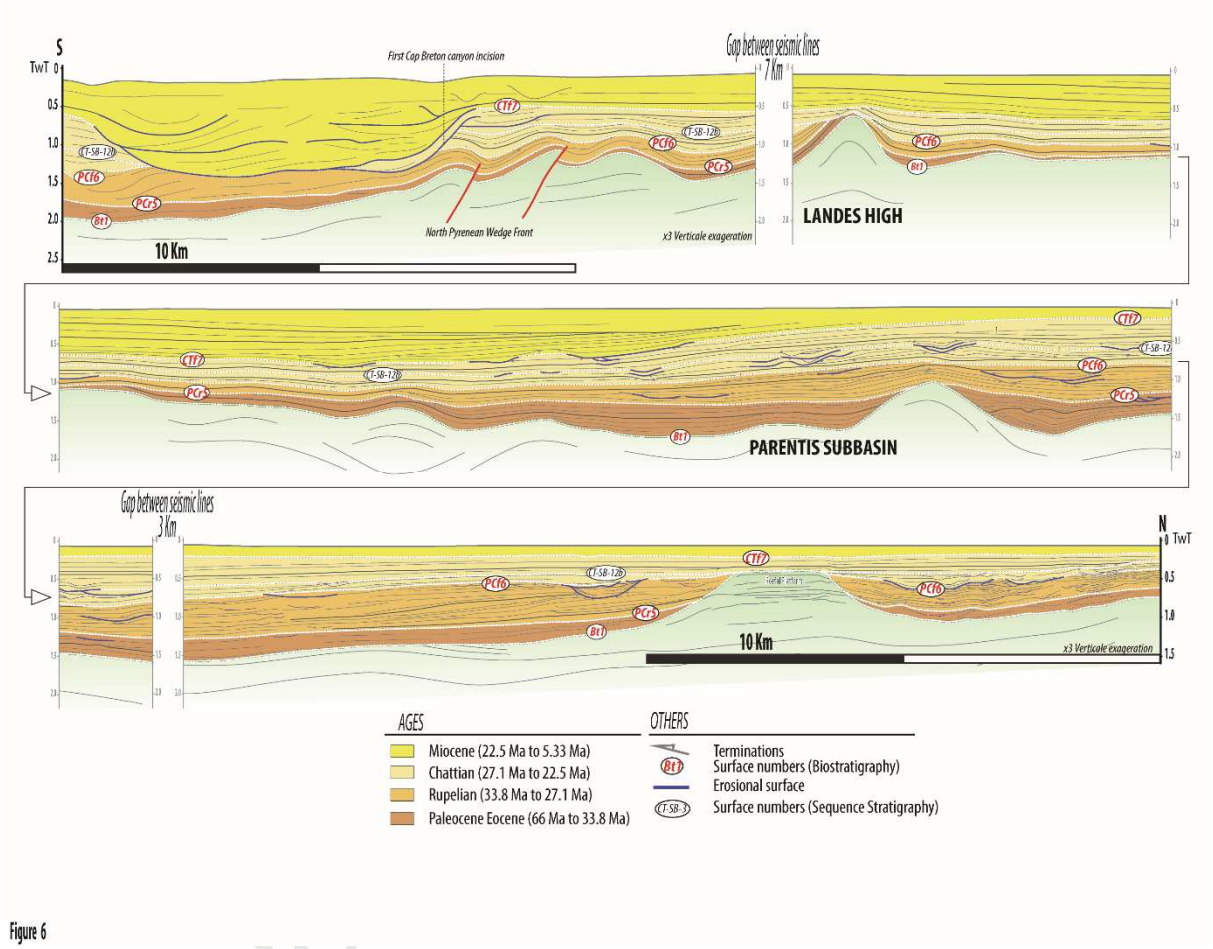

1396 Figure 6

1397 **Fig. 6**. Sequence stratigraphic and structural interpretation of the 'offshore shoreline-

1398 parallel' seismic line (see Fig. 2 for location).

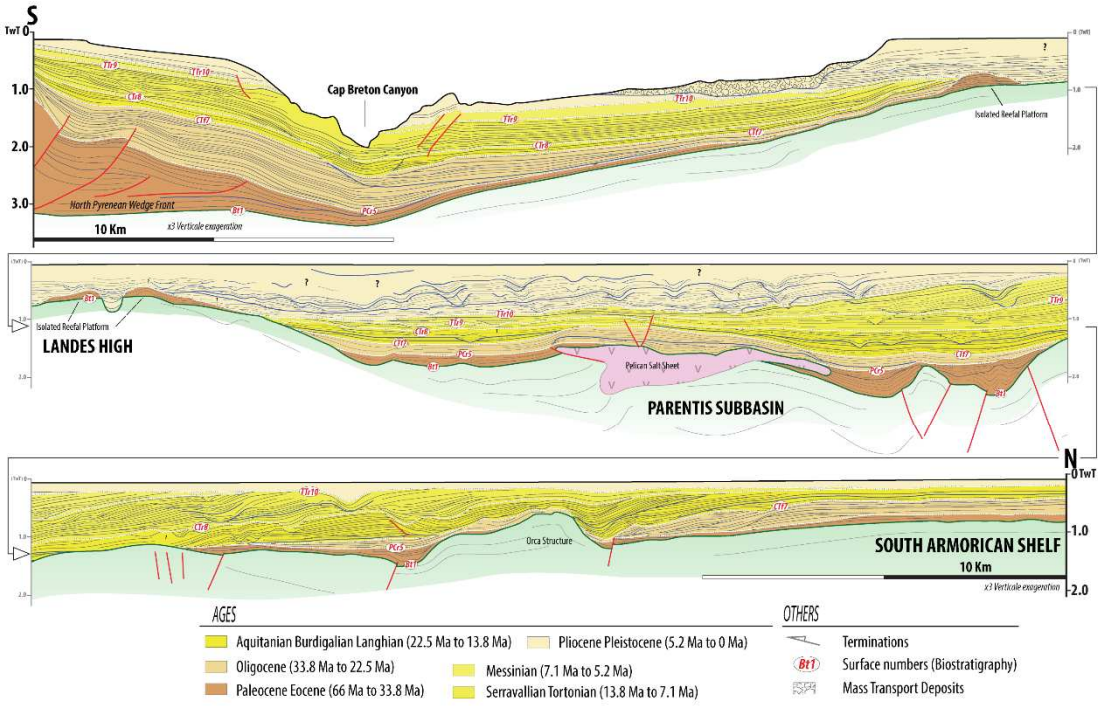

1399 **Figure 7**

1400 **Fig. 7**. Sequence stratigraphic and structural interpretation of the ECORS offshore seismic

1401 line (see Fig. 2 for location).

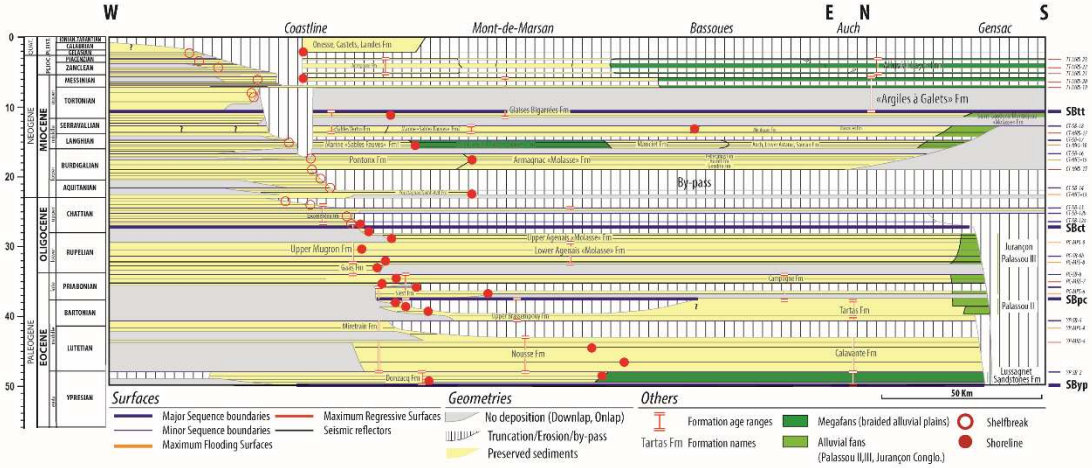

Figure 8

1402

1403 **Fig. 8**. Space-time stratigraphic (Wheeler) diagram of the Aquitaine Basin along a W-E-S

1404 transect from the near offshore to the Lannemezan Plateau.

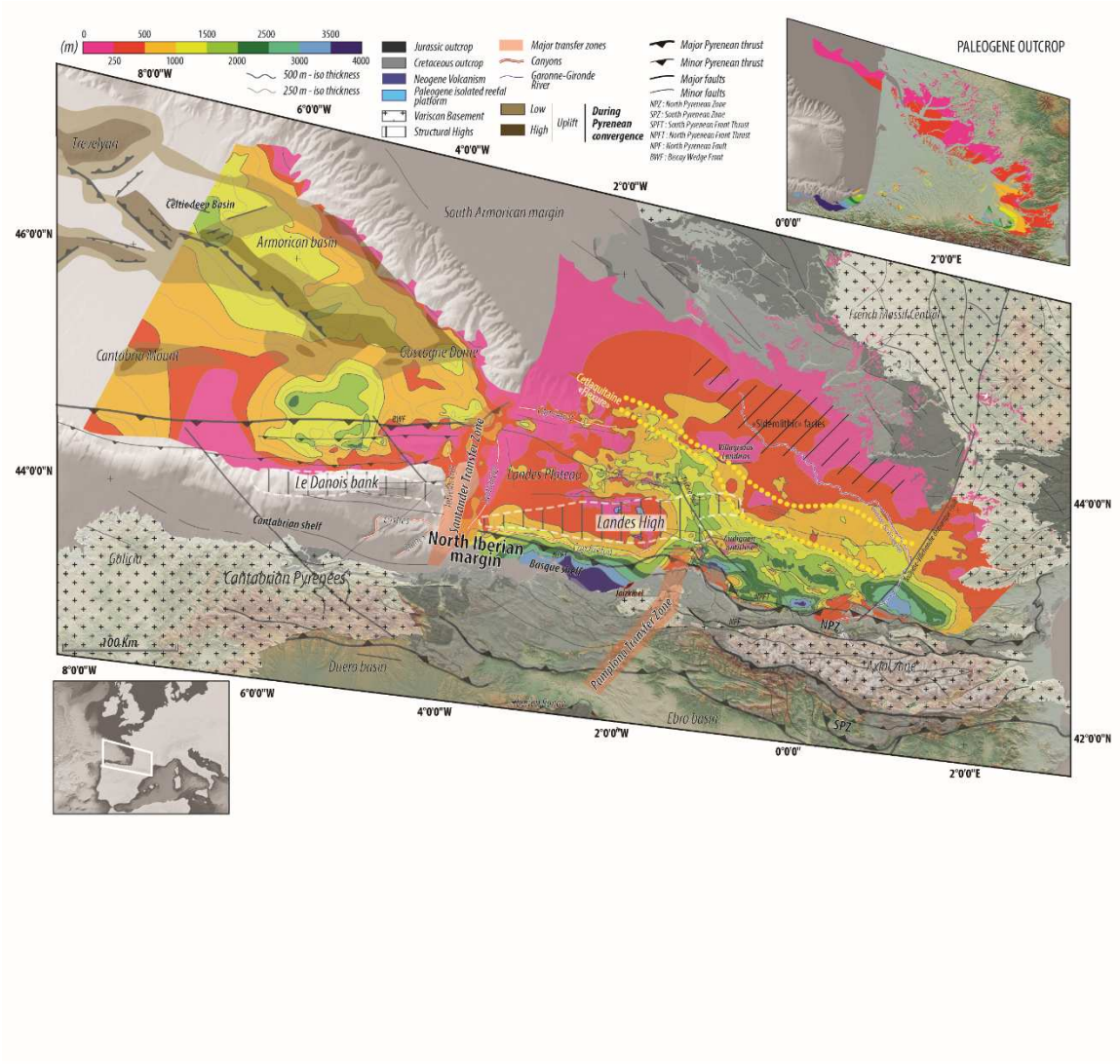

1405 **Figure 9**

1406 **Fig. 9**. Sediment thickness (isopach) map of the Palaeogene (66-23 Ma)

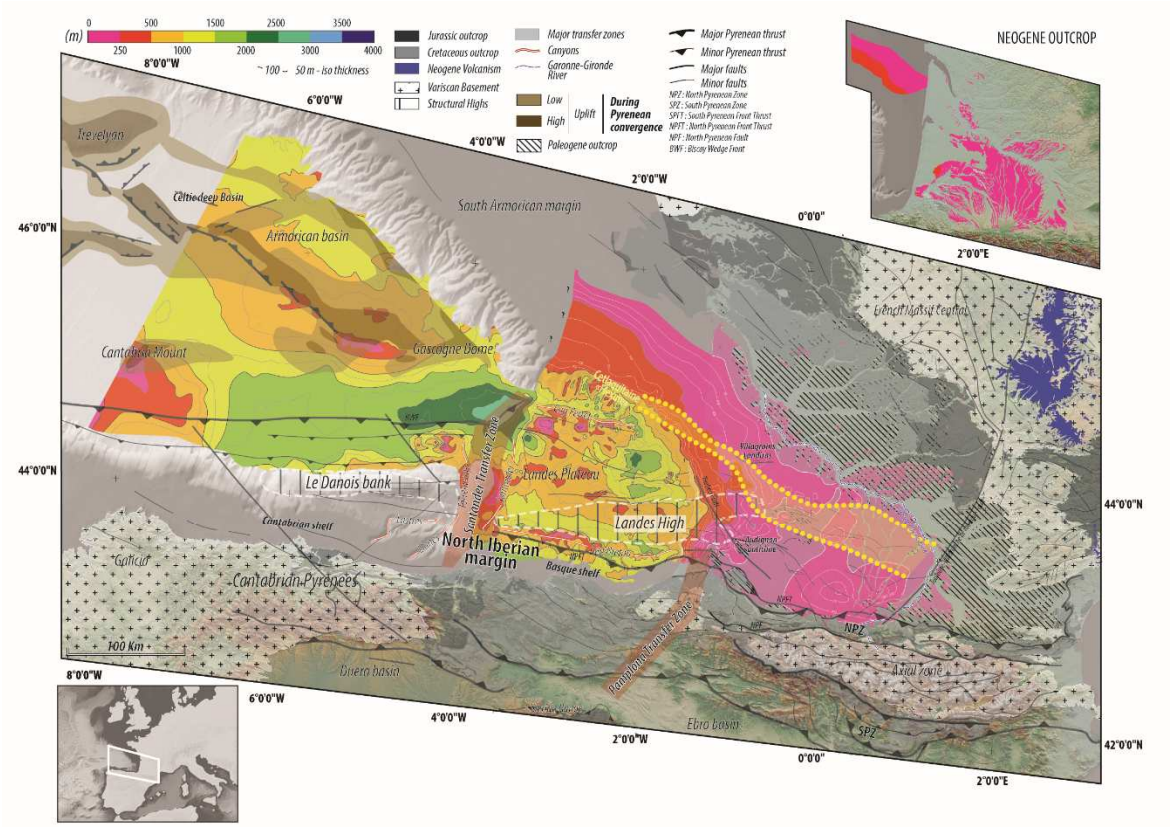

Figure 10

1408 **Fig. 10**. Sediment thickness (isopach) map of the Neogene (23-0 Ma)

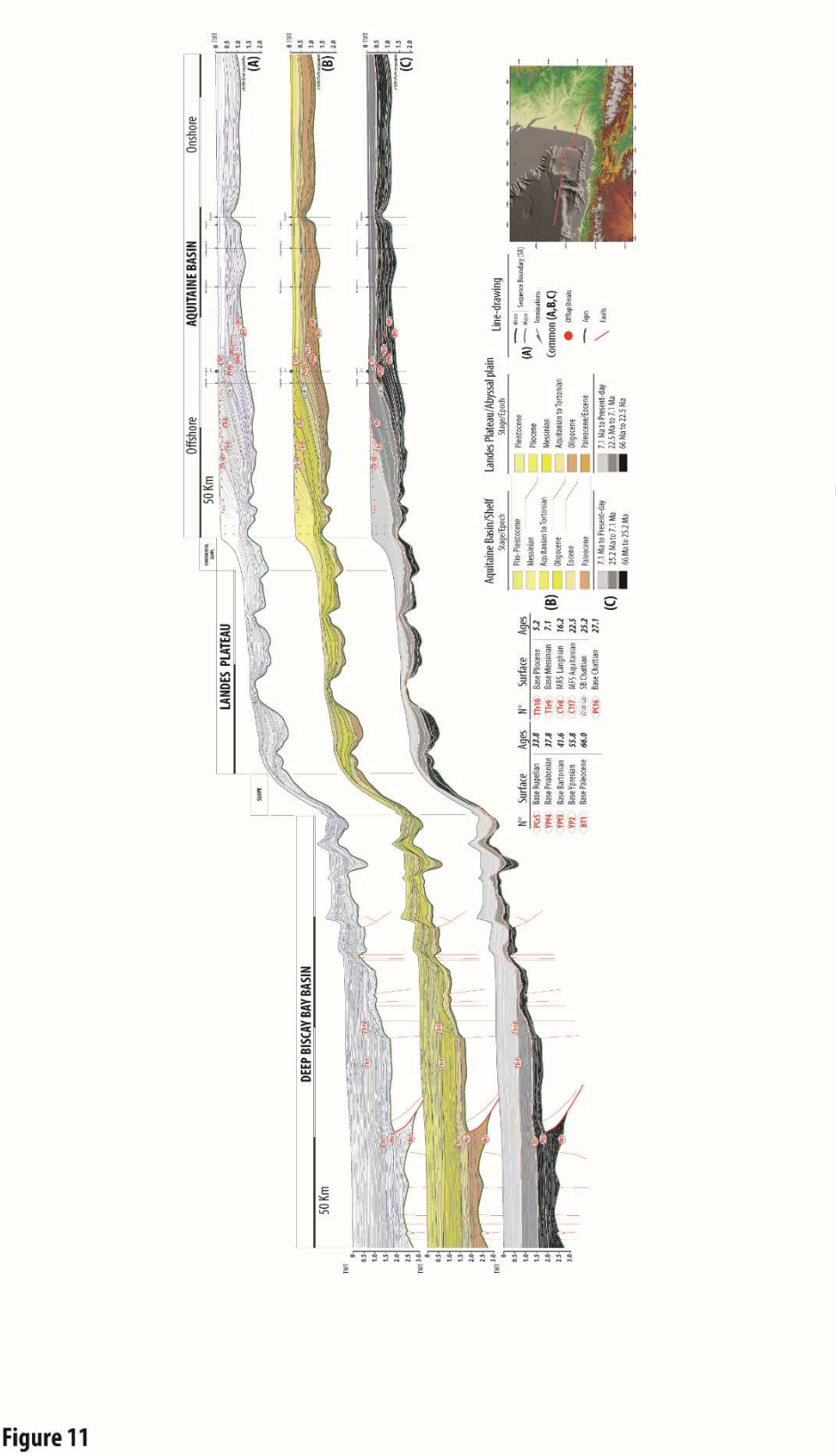

1411 **Figure 11**

1412 **Fig. 11**. East-West onshore-offshore regional seismic line from the Aquitaine Basin to the Bay

1413 of Biscay deep basin (see Fig. 2 for location). Due to the superimposition and truncation of

successive erosional surfaces on the shelf and slope or poor time-resolution in the deep basin, the two main discontinuities traced here do not strictly correspond to SBct and SBtt. The first main discontinuity (equivalent to SBct) is the last Chattian SB (CT-MFS-12b) truncating SBct on the shelf and slope and the MFS of the Aquitanian (CTf7) in the deep basin. The second main discontinuity (equivalent to SBtt) is the base Messinian MRS (TTr9) truncating the base Tortonian sequence boundary SBtt.

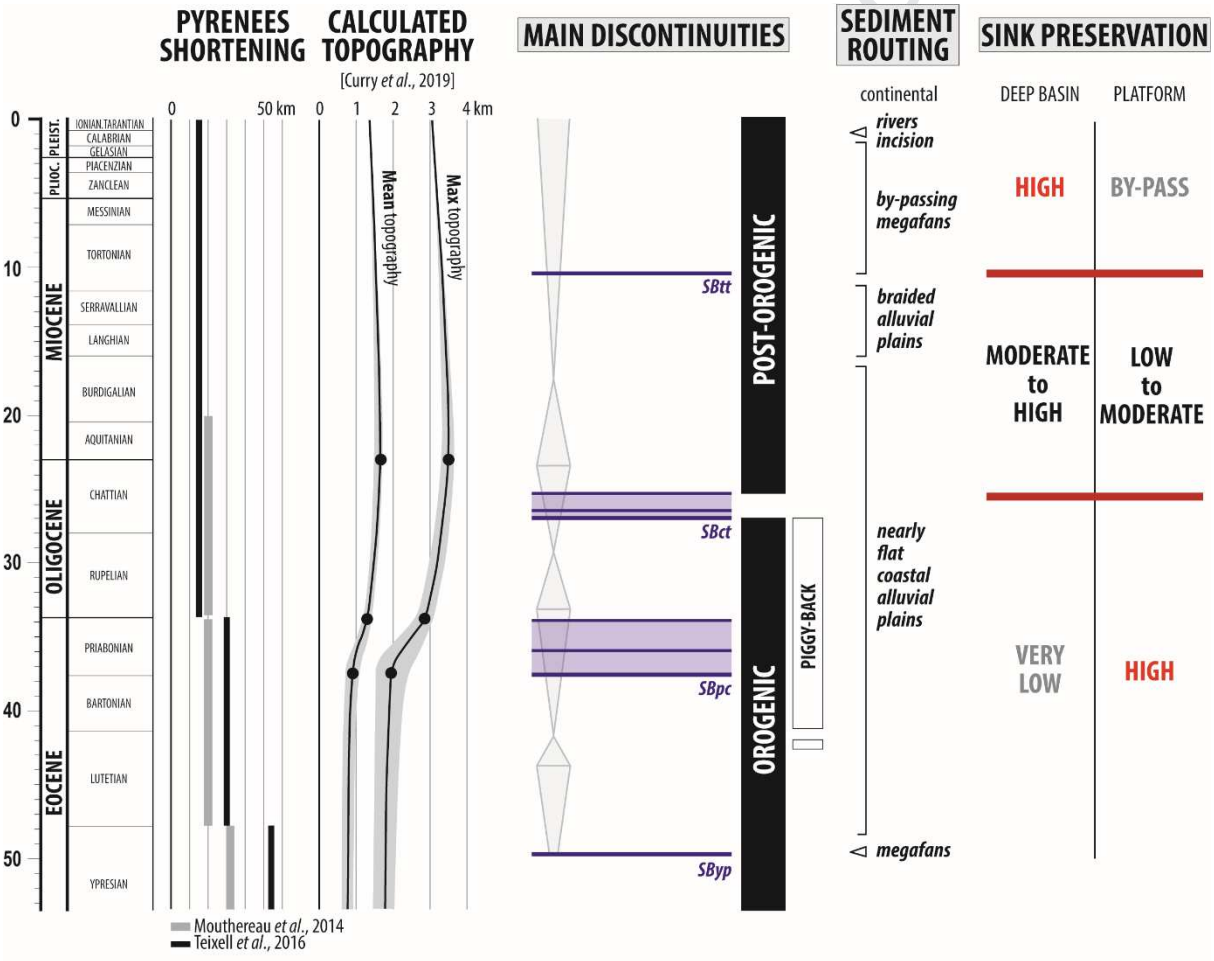

Figure 12

Fig. 12. Synthetic chart of the main events (deformation, topography, sediment routing) of the Aquitaine Basin to Bay of Biscay deep basin sedimentary system.

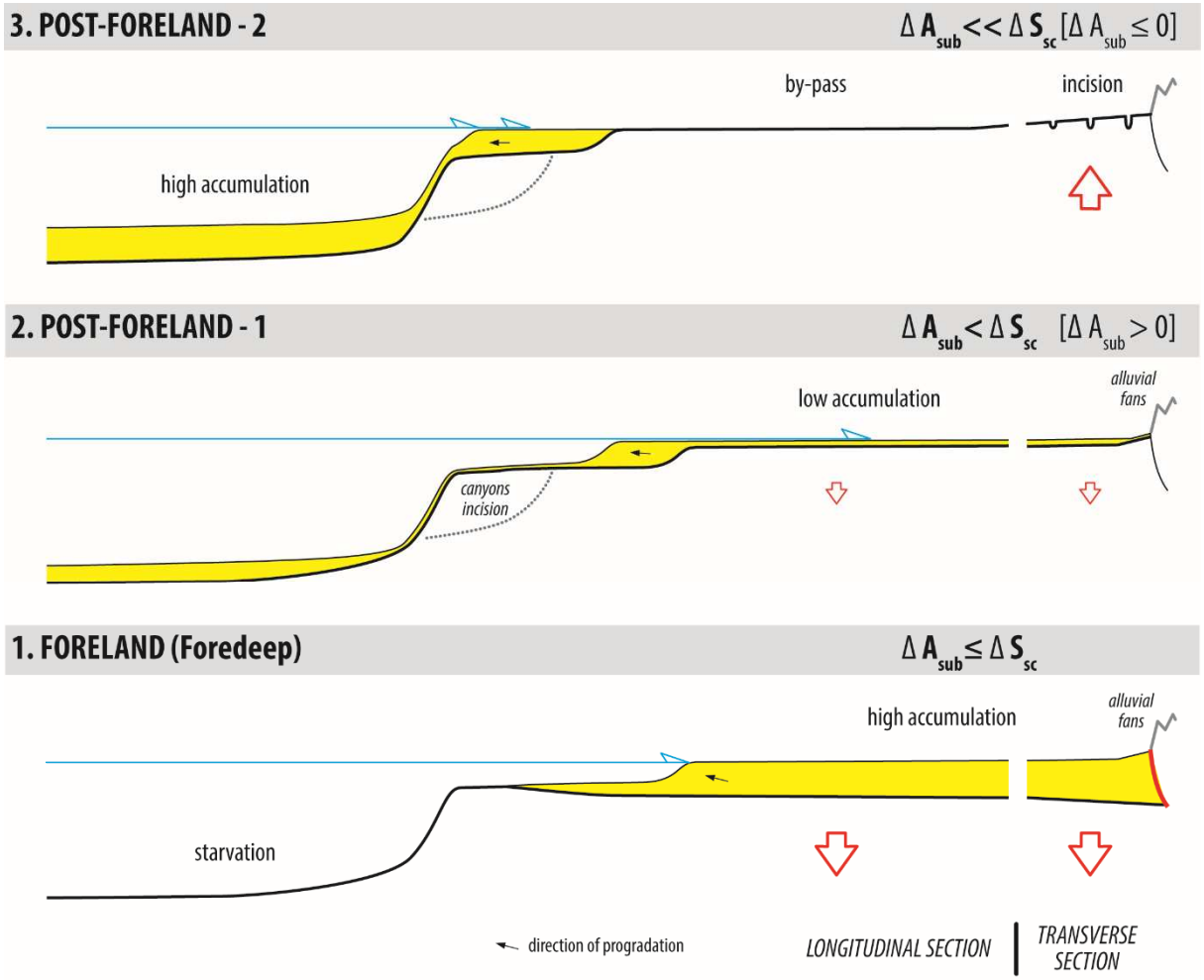

1423 **Figure 13**

1424 **Fig. 13**. A model of the sediment preservation and sediment routing system of the retro-

1425 foreland basin passing laterally to a passive margin.

1426

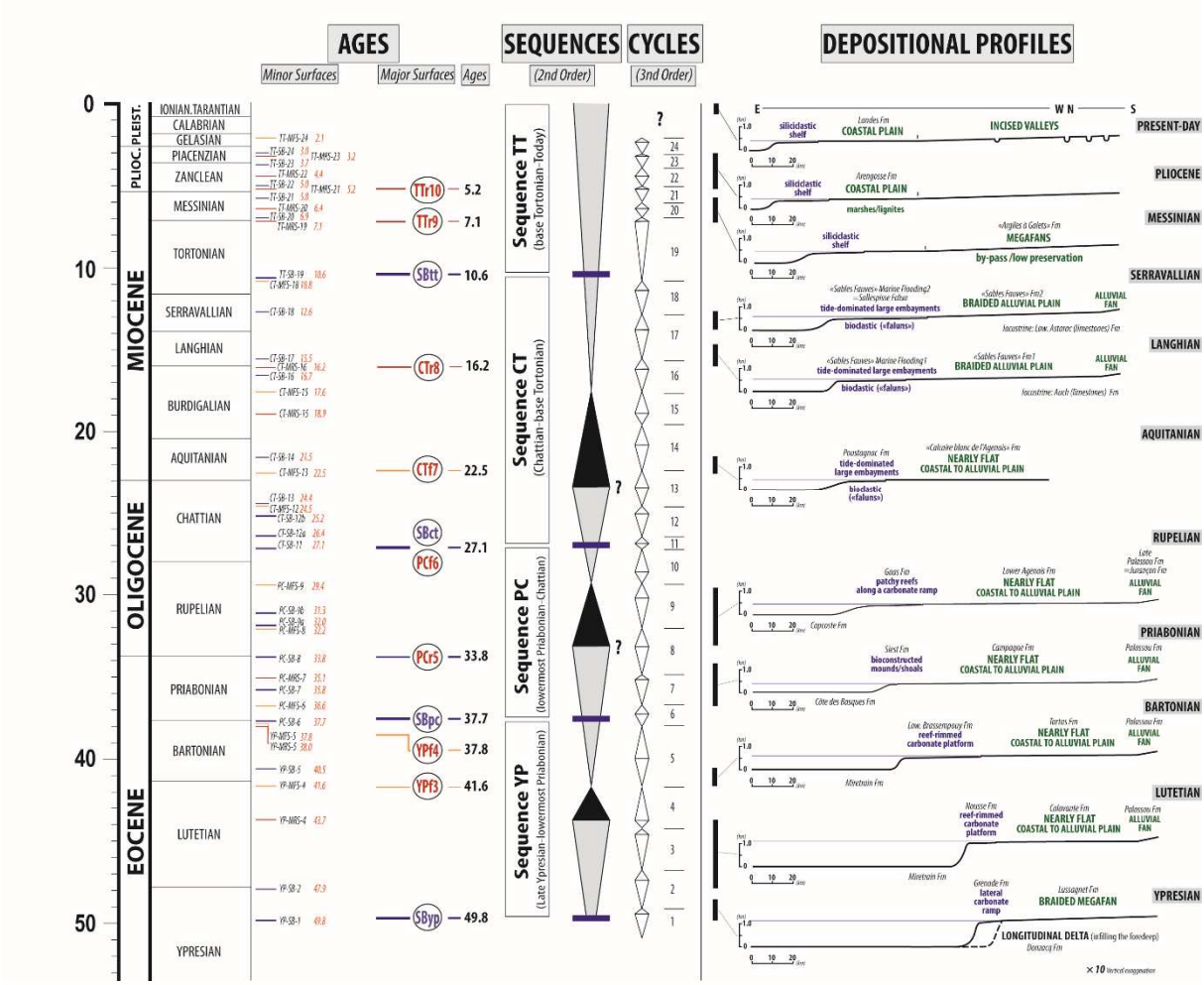

Table 1

1427

Table1. Chronostratigraphic framework of the different orders of sequences and related surfaces (see supplementary material 1 for age constraints) and evolution of the depositional profiles on the Aquitaine platform.

- A new chronostratigraphic and sequence stratigraphic framework
- Characterisation of successive deformations: age, wavelengths, causes
- Evolution of the sediment routing system: depositional profiles and topographies
- A sink preservation model based on the ratio vertical movements / sediment supply

Declaration of interests

☒ The authors declare that they have no known competing financial interests or personal relationships that could have appeared to influence the work reported in this paper.

☐The authors declare the following financial interests/personal relationships which may be considered as potential competing interests: